OPTICAL PROPERTIES OF MULTILAYER STACKS

A THESIS PRESENTED TO

THE SCHOOL OF GRADUATE STUDIES

ADDIS ABABA UNIVERSITY

IN PARTIAL FULFILMENT OF

THE REQUIREMENTS FOR THE DEGREE OF

MASTER OF SCIENCE IN PHYSICS

BY

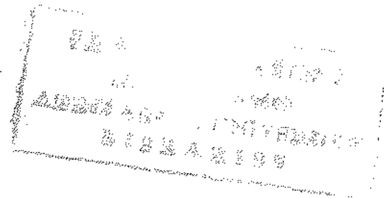

SOLOMON BENEBERU

ADDIS ABABA

JUNE 1997

DEDICATION

To

Alemtsehay Tesfaye and

Beneberu Meteke

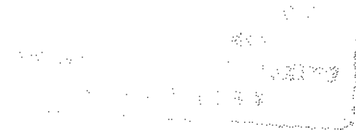

ACKNOWLEDGEMENT

I would like to express my deepest gratitude to Dr. Ulrich Stutenbaeumer my advisor, who gave his time, energy and advice with no reservations and by giving me a computer training. I also express my thanks to Dr. Thomas Eickhoff who gave me the solar cell samples and the reflectance spectra and data.

I extend my thanks to IPPS (International Programme in the physical Sciences UPPSALA university, Sweden) and to Dr. Bantikassagne Workalemahu who provided me with the PERKIN ELMER Lambda 19 for the measurement of transmittance spectra and other materials. I extend my thanks for the AAU graduate school who gave me a financial support, and I also express my thanks to the department of physics members. I also thanks Ato Tadesse Tassew for his good co-operation of giving important materials for my project work. I also have special thanks to Alemtsehay Tesfaye, Birtukan Tesfaye, Aberash Tesfaye, Anchinesh Tesfaye, Ato Asmamaw Yimer and his family, Ato Getahun G/Medhin and his family, Ato Tesfaye Gizaw and his family, Beneberu Meteke, Aselfech Reta, Ato Fekade T/ Berhan and his family, Ato Tawoke Gulilat, Ato Zerihun Tariku and his family, Ato Alemna Jaleta and Ato Belayneh Mesfin for their financial and material encouragement during my work. Above all, I praise you, GOD of my ancestors, You have given me wisdom and strength.

ADDIS ABABA
UNIVERSITY
LIBRARIES

Abstract

The optical properties of a-Si:H multilayer stacks are determined by comparing the measured reflectance and transmittance spectra with a computer simulation using simple dielectric function models. The samples were produced in the research center Juelich (Germany), where also the reflectance spectra were obtained in the spectral region between $4{,}000\ cm^{-1} <$ wavenumber $< 40{,}000\ cm^{-1}$. The transmittance spectra in the same spectral region for the same samples were done in the AAU spectroscopy laboratory. The obtained properties of the a-Si:H multilayer stacks, the layer thickness, the dielectric background and the band gap energy of the individual semiconductor materials are in good agreement with the reference values.

CONTENTS

1. INTRODUCTION 1

2. SIMULATION OF DIELECTRIC FUNCTIONS 5

2.1 Dielectric function 5

2.2 Constant Susceptibility 5

2.3 Harmonic oscillator 6

2.4 Drude susceptibility for free carriers 8

3. SIMULATION OF MULTILAYER STACKS 10

4. MEASURING TRANSMITTANCE AND REFLECTANCE 16

4.1 Double beam spectrometry 16

4.2 Measuring transmittance 17

5. TRANSMITTANCE AND REFLECTANCE SPECTRA OF a-Si:H MULTILAYER STACKS 18

5.1 TCO sample 20

5.2 TCOP sample 23

5.3 TCOPI1 sample 26

5.4 TCOPI2 sample 29

6. COMPUTER SIMULATION OF TRANSMITTANCE AND REFLECTANCE SPECTRA OF a-Si:H MULTILAYER STACKS 33

6.1 SCOUTFIT computer programme 33

6.2 Computer simulation of the reflectance spectrum of the TCO sample 35

6.3 Computer simulation of the transmittance spectrum of the TCO sample 38

6.4 Computer simulation of the reflectance spectrum of the TCOP sample 40

6.5 Computer simulation of the transmittance spectrum of the TCOP sample 43

6.6 Computer simulation of the reflectance spectrum of the TCOPI1 sample..........45

6.7 Computer simulation of the transmittance spectrum of the TCOPI1 sample......47

6.8 Computer simulation of the reflectance spectrum of the TCOPI2 sample..........49

6.9 Computer simulation of the transmittance spectrum of the TCOPI2 sample......51

7. DISCUSSION OF THE OPTICAL PROPERTIES OF a-Si:H MULTILAYER STACKS..........53

7.1 Discussion of the layer thickness..........53

7.2 Discussion of the optical parameters..........54

8. REFERENCES..........59

CONTENTS OF FIGURES AND TABLES

1. Figure 1 Schematic cross-section of a p-i-n, a-Si:H solar cell....................................3

2. Figure 2.1 Dielectric function of a group IV semiconductor including Silicon............6

3. Figure 2.2 Dielectric function of a highly p- doped Silicon in the infrared spectral range...9

4. Figure 3.1 Wave that acts at the interface between two layers................................11

5. Figure 3.2 Multiple reflection of stacks of layers..13

6. Figure 3.3 Multilayer stacks 14

7. Table 5.1 Samples used in the experiment...18

8. Figure 5.1 Transmittance spectrum of the TCO sample consisting of a glass substrate and a coated transparent conducting oxide layer.......................................20

9. Figure 5.2 Reflectance spectrum of he TCO sample 20

10. Figure 5.3 Absorption spectrum of the TCO sample calculated from the corresponding transmittance (figure 5.1) and reflectance spectrum (figure 5.2)......22

11. Figure 5.4 Transmittance spectrum of the TCOP sample consisting of a glass substrate and a coated transparent conducting oxide layer with an additional p-doped a-Si:H layer...23

12. Figure 5.5 Reflectance spectrum of the TCOP sample 23

13. Figure 5.6 Absorption spectrum of the TCOP sample calculated from the corresponding transmittance (figure 5.4) and reflectance spectrum (figure 5.5).....25

14. Figure 5.7 Transmittance spectrum of the TCOPI1 sample consists of a glass substrate, a coated TCO layer and an additional coated p and I- doped a-Si:H layer...26

15. Figure 5.8 Reflectance spectrum of the TCOPI1 sample......................................26

16. Figure 5.9 Absorption spectrum of the TCOPI1 sample calculated from the corresponding transmittance (figure 5.7) and reflectance spectrum (figure 5.8).....28
17. Figure 5.10 Transmittance spectrum of the TCOPI2 sample consisting of a glass substrate, a coated transparent conducting oxide layer and an additional p- and i-doped a-si:H layer.....29
18. Figure 5.11 Reflectance spectrum of TCOPI2 sample 29
19. Figure 5.12 Absorption spectrum of TCOPI2 sample calculated from the corresponding transmittance (figure 5.10) and reflectance spectra (figure 5.11).....32
20. Table 6.1 The layer stack of the TCO sample and the SCOUTFIT dielectric function models.....36
21. Figure 6.1 The reflectance and the SCOUTFIT simulated spectrum of the TCO sample 36
22. Table 6.2 SCOUTFIT optical parameters of the TCO sample simulated with a reflectance spectrum.....37
23. Table 6.3 The layer stack of the TCO sample and the SCOUTFIT dielectric function models.....38
24. Figure 6.2 The transmittance and the SCOUTFIT simulated spectrum of the TCO sample.....38
25. Table 6.4 SCOUTFIT optical parameters of the TCO sample simulated with the transmittance spectrum.....39
26. Table 6.5 The layer stack of the TCOP sample and the SCOUTFIT dielectric function model.....40
27. Figure 6.3 The reflectance and SCOUTFIT simulated spectrum of the TCOP sample.....41

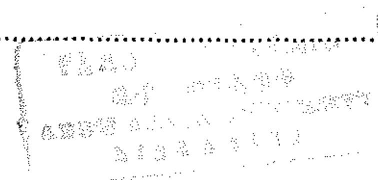

28. Table 6.6 SCOUTFIT optical parameters of the TCOP sample simulated with a reflectance spectrum 42
29. Table 6.7 The layer stack of the TCOP sample and the SCOUTFIT dielectric function models....................43
30. Figure 6.4 The transmittance and the SCOUTFIT simulated spectrum of the TCOP sample 43
31. Table 6.8 SCOUTFIT optical parameters of the TCOP sample simulated with a transmittance spectrum....................44
32. Table 6.9 The layer stack of the TCOPI1 sample and the SCOUTFIT dielectric function models....................45
33. Figure 6.5 The reflectance and the SCOUTFIT simulated spectrum for the TCOPI1 sample....................45
34. Table 6.10 SCOUTFIT optical parameters of the TCOPI1 sample simulated with a reflectance spectrum....................46
35. Table 6.11 The layer stack of the TCOPI1 sample and the SCOUTFIT dielectric function models....................47
36. Figure 6.6 The transmittance and the SCOUTFIT simulated spectrum for the TCOPI1 sample....................47
37. Table 6.12 SCOUTFIT optical parameters of the TCOPI1 sample simulated with a transmittance spectrum 48
38. Table 6.13 The layer stack of the TCOPI2 and the SCOUTFIT dielectric function models....................49
39. Figure 6.7 The reflectance and the SCOUTFIT simulated spectrum of the TCOPI2 sample....................49
40. Table 6.14 SCOUTFIT optical parameters of the TCOPI2 sample simulated with the reflectance spectrum....................50

41. Table 6.15 The layer stack of the TCOPI2 sample and the SCOUTFIT dielectric function models 51

42. Figure 6.8 The transmittance and the SCOUTFIT simulated spectra of the TCOPI2 sample 51

43. Table 6.16 SCOUTFIT optical parameters of the TCOPI2 sample simulated with the transmittance spectrum..52

44. Table 7.1 Layer thickness of the TCO, TCOP, TCOPI1 and TCOPI2 samples.....53

45. Table 7.2 The average values of the dielectric function model parameters obtained from the SCOUTFIT computer programme simulated spectrum and the referred values...56

1. INTRODUCTION

The photovoltaic effect was discovered more than 100 years ago. Since the demonstration of the crystalline Silicon (Si) p-n junction solar cell in 1954, photovoltaics and microelectronics have been closely linked. As Si microelectronics developed and expanded, there were similarly high hopes for terrestrial power generation by solar cells. By 1956, solar cells for terrestrial applications were produced for different purposes. [5]

The development of these photovoltaic cells within these years increases its efficiency in the laboratory demonstration. This improvements in output current, significant increases in output voltage and splitting of light among solar cells of different band gaps that waste less of the sun light input, are deeply connected with the density of the minority carriers generated by the absorbed light. The three most important ways for improving the minority-carrier generation are:

1) reducing the minority-carrier recombination rate.

2) trapping light in active layers.

3) increasing the intensity of light with concentrating optics.

In single-crystal Si and GaAs laboratory cells, respectively, one or both of the first two improvements have led to 23% and 24% efficient devices and inclusion of the third has given 26% and 28% efficient devices. Hydrogenated amorphous silicon (a-Si:H) alloy materials have led to 14% laboratory cell efficiencies using multiple band gaps and light trapping without light concentration. [3,14]

Another improvement of solar cells is to collect longer wavelength photons by absorption using stacked junctions of lower-energy gap semiconductors. The reason for this is that the energy gap in a-Si of 1.7-1.8 eV is higher than that of crystalline

solar cell semiconductors. Since thin films are produced by techniques such as CVD, MOCVD, molecular beam epitaxy, sputtering and ion plating which are already established for a wide variety of producing techniques, combining all these techniques together at low temperatures can establish a stack of layers for solar cell use. And progresses of material selection and economic feasibility studies are showing that an efficiency of 18% could be obtained with this structure by assuming a fill factor of 70% and an open circuit voltage of V_{oc}= 1.43V, obtained with different cell structures.[6] Thin films a-Si:H p-i-n solar cells are also good candidates for very cheap mass production of solar generators and therefore an interesting item for the electrical energy contribution specially in rural areas of developing countries like Ethiopia. For the future improvement of the conversion efficiency of a-Si:H p-i-n solar cells the knowledge of the optical properties of the individual layers of the layer stack system is of great importance. The determination of the reflectance and transmittance in the wavelength range $250< \lambda < 2500$nm (4000< wavenumber< 40,000cm^{-1}) for layer systems which creates the p-i-n structure of the a-Si:H solar cell, provides information of the optical constants of the different layers and their thickness.

A p-i-n structure a-Si:H thin film solar cell consists out of a glass substrate coated with a transparent conducting oxide (TCO) for connecting the front contacts. On top of this a p-doped a-Si:H layer followed by an intrinsic i-layer and n-doped layer is sputtered on the substrate. An additional metal back contact provides the second connecting contact of the solar cell.

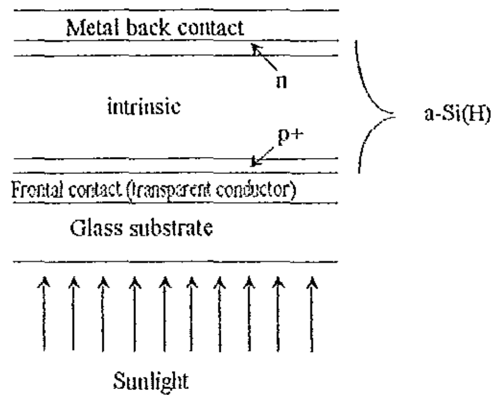

Figure 1. Schematic cross-section of a p-i-n a-Si:H solar cell.

The samples used in this thesis are transparent conducting oxide on a glass substrate (TCO), transparent conducting oxide on a glass substrate with an additional p-doped a-Si:H layer (TCOP), transparent conducting oxide on a glass substrate with an additional p-doped a-Si:H and an I-layer a-Si:H of thickness 50nm (TCOPI1) and transparent conducting oxide with p- and I- doped a-Si:H layer of thickness 380nm (TCOPI2). The samples are obtained from the Juelich research center (Germany). The reflectance measurements were done in the Juelich research center by using a Perkin Elmer Lambda 19 spectrometer and the transmittance measurement were done in the AAU spectroscopy laboratory by using the same samples and a similar apparatus. The optical properties of multilayer stacks obtained from transmittance measurements and the determination of the dielectric functions of the individual layers by using computer simulations were done for the first time in Addis Ababa University. In the measurement of the transmittance spectra the Perkin Elmer Lambda 19 UV/VIS/NIR double beam spectrometer was used and the measurement was done at room temperature and over the wavelength range of 250nm < λ < 2500nm or over the wavenumber range of 4000cm^{-1} < wavenumber < 40,000cm^{-1}.

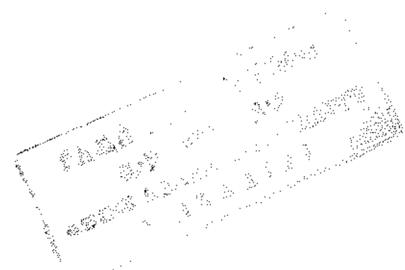

In chapter 2, important physical models to determine the dielectric function of a substrate are discussed. In chapter 3, the complex reflectance and transmittance and the optical interaction at the interface between two layers and multilayer stacks are discussed. In chapter 4, the experimental set up used in the investigation and the procedure is explained. In chapter 5, the reflectance and transmittance spectra of the TCO, TCOP, TCOPI1 and TCOPI2 samples are presented. In chapter 6, the SCOUTFIT computer simulation programme is explained, the simulated spectra are presented and the fitting parameters are tabulated. In chapter 7, the results of the simulation of the measured spectra and the dielectric function models for the individual layer stacks are discussed and finally , the reference material is listed .

2. SIMULATION OF DIELECTRIC FUNCTIONS

2.1 Dielectric function

The electric field of light which interacts with a material object is connected with the polarization of the material. The polarization $\vec{P}$ is produced by the electric field that is acting in a homogeneous material and is related by the electric susceptibility χ. Mathematically this can be expressed as

$$\vec{P} = \varepsilon_0 \chi \vec{E} \qquad (2.1)$$

The dielectric displacement $\vec{D}$ and the electric field $\vec{E}$ is related by the dielectric function ε

$$\vec{D} = \varepsilon_0 \varepsilon \vec{E} \qquad (2.2)$$

connecting ε and χ as:

$$\varepsilon = 1 + \chi \qquad (2.3)$$

2.2 Constant susceptibility

Figure 2.1 shows the dielectric function for the infrared region (IR), visible region (VIS) and ultraviolet spectral region (UV) for a group IV semiconductor. The very strong structure in the ultraviolet region is due to electronic interband transitions. In the infrared region, the dielectric function can only be noticed by a constant dielectric background. Thus the optical properties in the infrared region can be described by a constant and real dielectric function ε_∞.

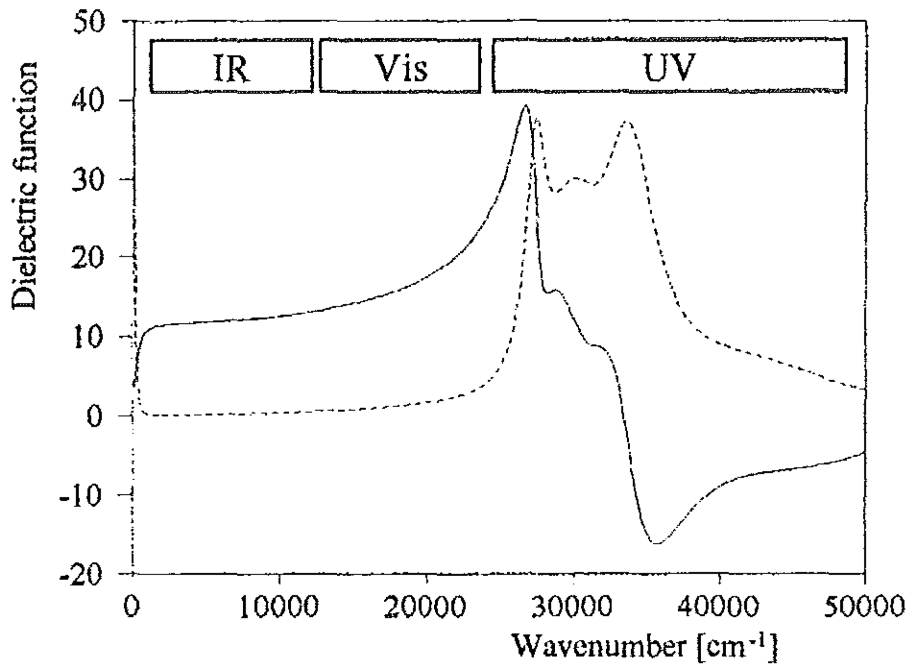

Figure 2.1 Dielectric function of a group IV semiconductor like Silicon. The dotted line represents the real part, the dashed line the imaginary part of the dielectric function.

2.3 Harmonic oscillator

Microscopic vibrations which consider the movement of nuclei of atoms have their resonance frequency mostly in the infrared region. The frequency depends on the mass of the oscillating atomic nuclei and the strength of the bonding between them. The susceptibility describing such microscopic vibrations can be expressed in the form of

$$\chi_{harmonic\,oscillator} = \frac{\Omega_P^2}{\Omega_{TO}^2 - \tilde{\nu}^2 - i\tilde{\nu}\Omega_\tau} \qquad (2.4)$$

where Ω_p is the oscillator strength, Ω_τ the damping and Ω_{To} the resonance position. Another example to use this simple oscillator model as a model to simulate the

dielectric function of a material is the band-to-band transition near the energy band gap of a semiconductor or an insulator. The corresponding resonant frequency depends on the energy position (E_g) of the band gap, which separates the valence from the conduction band [20]. For glass, the resonance frequency would be in the ultraviolet spectral region [17].

2.4 Drude susceptibility for free carriers

In highly doped semiconductors charge carriers are set free by donors or acceptors by a small amount of exciting energy in the infrared spectral energy region. Thus this charge carriers (electrons or holes) can be accelerated by an applied electric field. The susceptibility of these free charge carriers is given in the Drude model [1] by

$$\chi_{Drude} = -\frac{\Omega_P^2}{\tilde{\nu}^2 + i\tilde{\nu}\Omega_\tau} \tag{2.6}$$

where Ω_P is the plasma frequency given by the expression

$$\Omega_P^2 = \frac{ne^2}{\varepsilon_0 m} \tag{2.7}$$

and n is the volume density of the charge carriers, e and m are the charge and the effective mass of the charge carriers respectively. The dielectric function for highly p-doped silicon can be calculated as [1]

$$\varepsilon = \varepsilon_\infty + \chi_{Drude} \tag{2.8}$$

$$\varepsilon = \varepsilon_\infty - \frac{\Omega_P^2}{\tilde{\nu}^2 + i\tilde{\nu}\Omega_\tau} \tag{2.9}$$

with $\varepsilon_\infty = 11.7\text{cm}^{-1}$; $\Omega_p = 1800\text{cm}^{-1}$; $\Omega_\tau = 500\text{cm}^{-1}$

Figure 2.2 displays the dielectric function of a highly p-doped silicon crystal in the infrared spectral region [1]. For wavenumbers below 2000cm^{-1} the Drude model contributes to an abrupt change for the real and imaginary part of the dielectric function. Above 2000cm^{-1} the constant dielectric background ε_∞ defines the dielectric function of the material in the infrared spectral region. Therefore it is possible to determine the dielectric function of highly p-doped silicon in the infrared spectral region to good estimation by using a constant susceptibility and the Drude model.

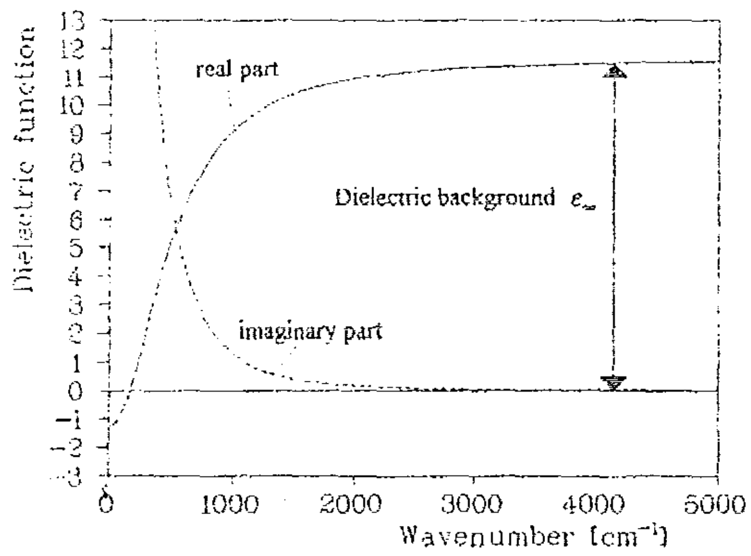

Figure 2.2. Dielectric function of a highly P-doped Silicon in the infrared spectral region.

3. SIMULATION OF MULTILAYER STACKS

The measured reflectance and transmittance spectra for the investigated multilayer stacks have to be analyzed to get the optical parameters of the individual layers. Therefore the complex layer stack system has to be separated into a more easily describeable system out of one interface only. The way it is done by the SCOUTFIT computer programme, which was used to analyze the data, is described in the following. [1]

The complex amplitude of the reflection and transmission coefficient can be determined by using a product of matrices. The matrix element describes the transformation of two plane waves travelling in opposite directions within the films. In different substrates of film arrangements it is possible to determine the reflection coefficient $R = rr^*$ and the transmission coefficient $T = tt^*$.

For a light wave, which is travelling in homogeneous media, the electric field for a plane wave by Maxwell's equation can be written as

$$\vec{E} = \vec{E}_0 \exp(i(\vec{K} \bullet \vec{r} - \omega t)) \tag{3.1}$$

where E_0 is the amplitude, K is the wavevector, r is the displacement and ω is the angular frequency of the wave.

For non-magnetic media this can take another form under the following approach

$$\vec{K} \bullet \vec{K} = \frac{\vec{\omega}}{C_0} \bullet \frac{\vec{\omega}}{C_0} \varepsilon(\omega) = \frac{\omega^2}{C_0^2} \varepsilon(\omega) \tag{3.2}$$

where C_0 is the speed of light in free space and $\varepsilon(\omega)$ is the dielectric function. In a more empirical form the above formula can be expressed as

$$\vec{K} \bullet \vec{K} = (\frac{2\pi}{\lambda_0})^2 \varepsilon(\omega) = k_0^2 \varepsilon(\omega) \tag{3.3}$$

Where λ_0 is the wavelength of light in vacuum and $K_0 = \frac{2\pi}{\lambda_0}$ is the wavevector in vacuum. Substituting equation (3.3) of the wavevector part in equation (3.1) one obtains that

$$\vec{E} = \vec{E_0}\exp(i(\vec{K}\bullet\vec{r} - \omega t))$$
$$= \vec{E_0}\exp(i(\sqrt{\varepsilon(\omega)}\vec{K_0}\bullet\vec{r} - \omega t))$$

Introducing in the above equation the complex index of refraction

$$n + i\kappa = \sqrt{\varepsilon(\omega)} \qquad (3.4)$$

gives the following equation

$$\vec{E} = \vec{E_0}\exp(i((n+i\kappa)\vec{K_0}\bullet\vec{r} - \omega t))$$
$$= \vec{E_0}\exp i(n\vec{K_0}\bullet\vec{r} - \omega t)\exp(-\kappa\vec{K_0}.\vec{r}) \qquad (3.5)$$

Equation (3.5) is a plane wave which is decaying exponentially with an intensity constant of absorption $K = 2\kappa k_0 = 4\pi\kappa\tilde{\nu}$.

Consider the wave which acts at the interface between two layers:

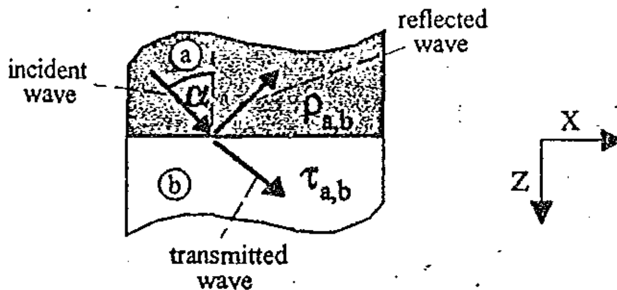

Figure 3.1 Wave at the interface between two layers

For the waves at the boundaries the treatment is done by Fresnel equations (figure 3.1). The light rays which are incident on the surface of the two media are partly reflected and partly transmitted and this can be evaluated by using the boundary conditions for electric and magnetic fields. $\rho_{a,b}$ is the amplitude of the reflection coefficient and $\tau_{a,b}$ is the amplitude of the transmission coefficient, both depend on the index of refraction of the different layers. Consider that the wavevector for the medium 'a' has a real index of refraction n_a, from our previous equation (3.2)

$\vec{K} = \frac{\vec{\omega}}{C_0}\sqrt{\varepsilon(\omega)}$ for the x-component of the wavevector it can be written in the form

$$K_X = \frac{\omega}{C_0} n_a \sin\alpha$$

where $\sqrt{\varepsilon(\omega)} = n_a \sin\alpha$

And the z-component of the wavevector is the same as:

$$K_z = \frac{\omega}{C_0}\sqrt{\varepsilon(\omega) - n_a^2 \sin^2\alpha} = \frac{\omega}{C_0}\widetilde{N} \quad (3.7)$$

where $\widetilde{N}$ is the complex index of refraction and α is the angle of incidence

$$\widetilde{N} = \sqrt{\varepsilon(\omega) - n_a^2 \sin^2\alpha}$$

Also, the complex index of refraction $\widetilde{N} = N + iK$, with its real part N(ω) and its imaginary part K(ω), cannot exist separately. To determine the two parts of $\widetilde{N}$, two different methods are used:

a) The first method is to carry out reflection and transmission measurements for all frequencies for normally incident light.

b) The second method is to measure either reflection or transmission at all frequencies, from zero to infinity and then calculating the phase of the complex-amplitude coefficient and applying it to the Kramers-Kronig transformation, which considers the internal relation between N and κ.[11]

Consider the S-polarization of light which is caused by the transverse electric field wave, in which the electric field is parallel to the surface of the stacks, and the P-polarization in which the transverse magnetic field wave is parallel to the surface of the stacks. Using the generalised index of refraction, so that the amplitude of transmission and reflection coefficients become to $\rho_{a,b}$ and $\tau_{a,b}$, then the S and P-polarization can be written in the form:

S-polarization: $\rho_{ab}=\frac{\tilde{N}_a-\tilde{N}_b}{\tilde{N}_a+\tilde{N}_b}$ $\qquad \tau_{ab}=\frac{2\tilde{N}_a}{\tilde{N}_a+\tilde{N}_b}$ (3.8)

P-polarization: $\rho_{ab}=\frac{\tilde{N}_a/\varepsilon_a-\tilde{N}_b/\varepsilon_b}{\tilde{N}_a/\varepsilon_a+\tilde{N}_b/\varepsilon_b}$ $\qquad \tau_{ab}=\frac{2\tilde{N}_a/\varepsilon_a}{\tilde{N}_a/\varepsilon_a+\tilde{N}_b/\varepsilon_b}$

At the interface of the layers inside a stack there is multiple reflection.

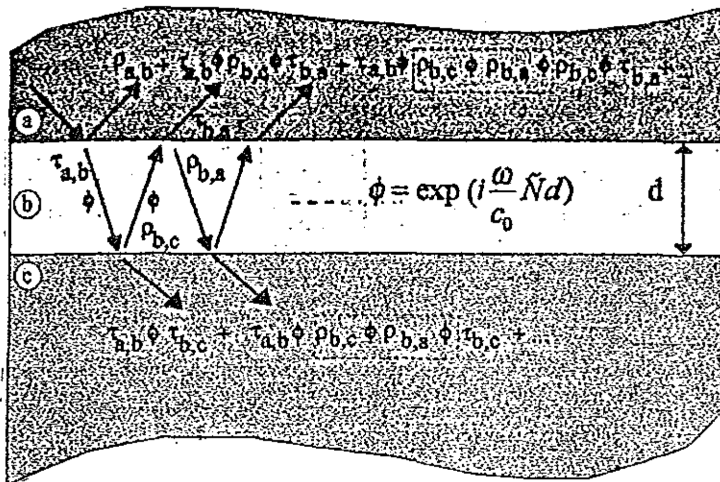

Figure 3.2 Multiple reflection inside a layer stack system.

In the above figure 3.2 for multiple reflection inside a layer stack system, the amplitude of reflection and transmission of a layer are found by using the geometric series of the partial wave contribution which is expressed in the form:

In medium 'a' $\rho_{a,b}+\tau_{a,b}\phi\rho_{b,c}\phi\tau_{b,a}+\tau_{a,b}\phi\underline{\rho_{b,c}\phi\rho_{b,a}}\phi\rho_{b,c}\phi\tau_{b,a}+\dots$.

In medium 'c' $\tau_{a,b}\phi\tau_{b,c}+\tau_{a,b}\phi\underline{\rho_{b,c}\phi\rho_{b,a}}\phi\tau_{b,c}+\dots$

The multiplied reflected contributions contain powers of the underlined terms and this underlined terms are used as a denominator by combining it with the geometric

series, and since the transmission and reflection are sum up to unity then the denominator will be

$$1-\rho_{b,c}\phi\rho_{b,a}\phi$$

Neglecting third order terms from medium 'a' and second order terms from medium 'c',[1] the amplitude of the reflection coefficient is

$$r_{a,b}=\rho_{a,b}+\frac{\tau_{a,b}\phi\rho_{b,c}\phi\tau_{b,a}}{1-\rho_{b,c}\phi\rho_{b,a}\phi} \tag{3.9}$$

and the amplitude of the transmission coefficient is

$$t_{a,b}=\frac{\tau_{a,b}\phi\tau_{b,c}}{1-\rho_{b,c}\phi\rho_{b,a}\phi} \tag{3.10}$$

The above expression (3.9) and (3.10) can be obtained by using the product of matrices [7].

The complex multilayer stacks can be reduced by repeating the above method with the last layer as shown in the figure below.

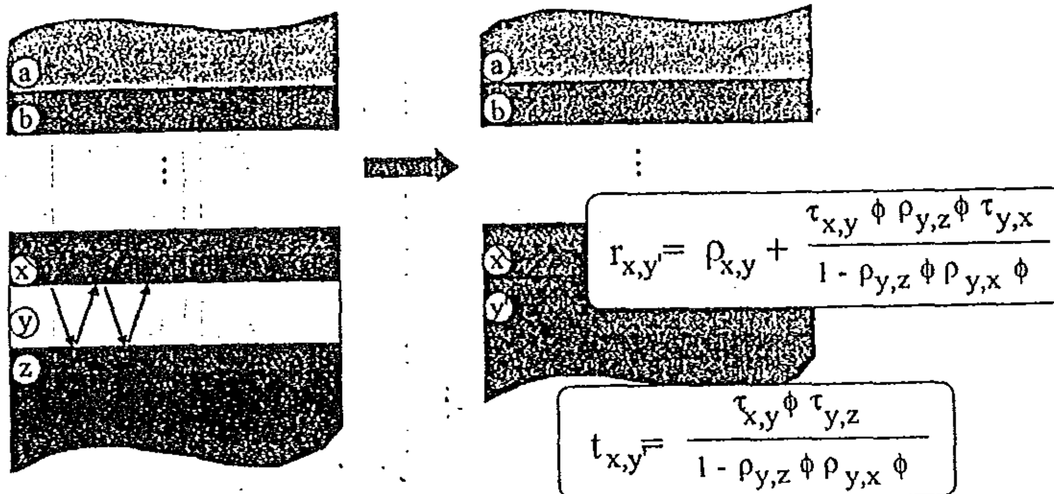

Figure 3.3 Method to reduce a finite layer stack system into a smaller stack.

A stack is a pile of plane-parallel layers between two halfspaces, that is the top and bottom halfspaces. Consider a light wave incident from the top halfspace onto the first

layer at an angle. A real index of refraction is to be assumed for the top halfspace and for all the individual layers. The reflection and transmission take place according to Fresnel's equations. The above problem is solved by summing up all the partial waves to the total transmitted and reflected radiation. In figure 3.2, it is possible to observe multiple reflections, and the transmission and reflection coefficients for the combination of layers inside the figure is given by equation (3.9) and (3.10). Based on the above condition, starting at the back side of the layer stack, the last layer and the bottom halfspace are combined to a new 'quasi'-halfspace of figure 3.3, which is combined with the next layer until the layer stack system is completed. Finally, the amplitudes of the reflected and transmitted waves are squared to give the corresponding intensities in the form of the equation:

$$R = |r_{x,y}|^2 = |\rho_{x,y}|^2 + \frac{|\tau_{x,y}|^2 \phi^4 |\rho_{y,z}|^2 |\tau_{y,x}|^2}{1 - |\rho_{y,z}|^2 \phi^4 |\rho_{y,x}|^2} \tag{3.11}$$

$$T = |t_{x,y}|^2 = \frac{|\tau_{xy}|^2 \phi^4 |\tau_{y,x}|^2}{1 - |\rho_{y,z}|^2 \phi^4 |\rho_{y,x}|^2} \tag{3.12}$$

4. MEASURING TRANSMITTANCE AND REFLECTANCE

4.1 Double beam spectrometer

The reflectance and transmittance measurements were done with the Perkin Elmer Lambda 19 UV/VIS/NIR double beam spectrometer. It measures the ratio of the intensities of the sample beam to that of the intensity of the reference beam. The spectral ranges are:

ultraviolet (UV) region from 185nm upto 320nm, Visible region from 320nm upto 860nm and near infrared (NIR) region from 860nm upto 3200nm.

In the ultraviolet spectral region two monochromators in series in littrow configuration are used and the optical filters are programmed to change automatically when the monochromator is slewing. For the near infrared spectral region two monochromators with gratings and programmed optical filters are present and they are changing automatically when the monochromator is slewing. The holographic gratings for the ultraviolet and visible region is 1440lines/mm and for the near infrared is 360lines/mm and the beam separation in the sample compartment is 100mm.

The light source for the ultraviolet spectral region is a deuterium lamp, for the visible and near infrared region a tungsten-halogen lamp and there is an automatic source change when the monochromator is slewing.

The photodetectors used in the ultraviolet and visible ranges are a photomultiplier and a lead sulphide (PbS) detector for the near infrared range and the detectors are changed automatically when the monochromator is slewing.

The important parts of the LAMBDA 19 spectrometer system are:

1. main compartment of the spectrometer
2. two transmittance sample holders
3. personal computer with plotter

4.2 Measuring transmittance

To measure the near normal incidence transmittance the LAMBDA 19 spectrometer normal compartment is used by the following procedures:

a. The spectrometer is switched on for 20 minutes until the lamp reaches thermal equilibrium.

b. Putting the sample holder in its exact position of the sample beam.

c. Doing the instrument background correction. The background correction is calculated by using the formula

$$BC = \frac{I_s}{I_r}$$

where I_s is intensity of sample beam
I_r is intensity of the reference beam

d. Installing the sample on the transmittance holder and measuring the value, then the value of the transmittance is the result of

$$T = \frac{F_r}{BC}$$

where F_r is the value measured by the apparatus. [8,9,10]

5. TRANSMITTANCE AND REFLECTANCE SPECTRA OF a-Si:H MULTILAYER STACKS

The measurements of the transmittance and reflectance spectra for the same samples were done in two laboratories. The transmittance measurements in the AAU laboratory by using a Perkin Elmer LAMBDA 19 UV/VIS/NIR spectrometer and the reflectance measurements in Juelich research center (Germany) by using the same apparatus and the same samples. The measurements in both laboratories were done in the wavenumber range of $4000cm^{-1}$ < wavenumber < $40{,}000cm^{-1}$ ($250nm < \lambda < 2500nm$). The samples used during the experiments are tabulated below.

Sample Name	Sample layers	Thickness [18]
TCO	glass + TCO (Transparent Conducting Oxide)	glass: 1mm TCO: 70nm
TCOP	glass + TCO + p-doped a-Si:H	p-layer: 15nm
TCOPI1	glass + TCO + p-and I-layer a-Si:H	I-layer: 50nm
TCOPI2	glass + TCO + p- and I-layer a-Si:H	I-layer: 380nm

TABLE 5.1 Samples used in the experiments.

The glass/TCO sample is made out of a glass substrate and a coated transparent conducting oxide (TCO) layer. The TCOP sample is made out of glass and a transparent conducting oxide layer coated with a p-doped a-Si:H layer. The TCOPI sample is made out of glass and a transparent conducting oxide layer, coated with a

P-doped a-Si:H layer and coated with an additional intrinsic (I)-layer out of a-Si:H. In this experiment two different thicknesses of the I-layer were used. The first one is the TCOPI1 sample and the thickness of the I-layer is 50nm the second one is the TCOPI2 sample and the thickness of the I-layer is 380nm.

5.1 TCO sample

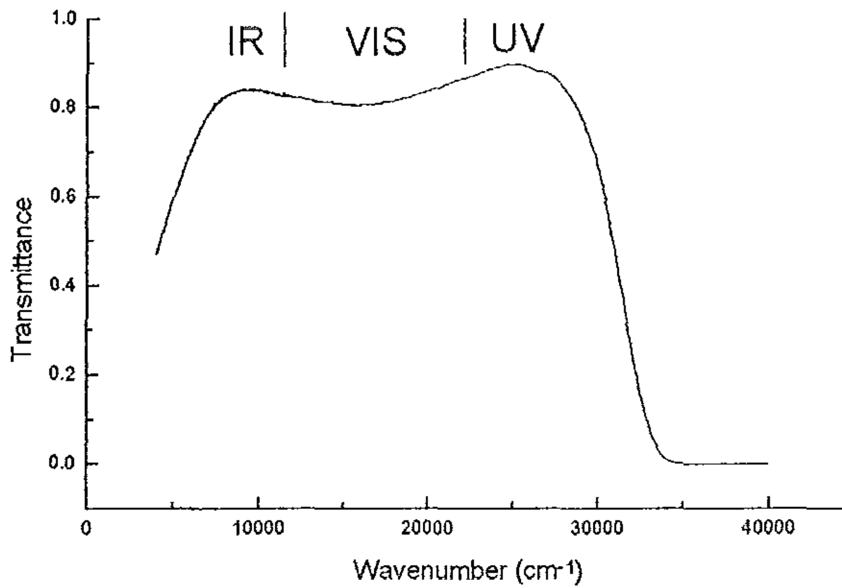

Figure 5.1 Transmittance spectrum of the TCO sample (consisting of a glass substrate and a coated transparent conducting layer). Indicated are the (IR) infrared, (VIS) visible and (UV) ultraviolet part of the spectrum.

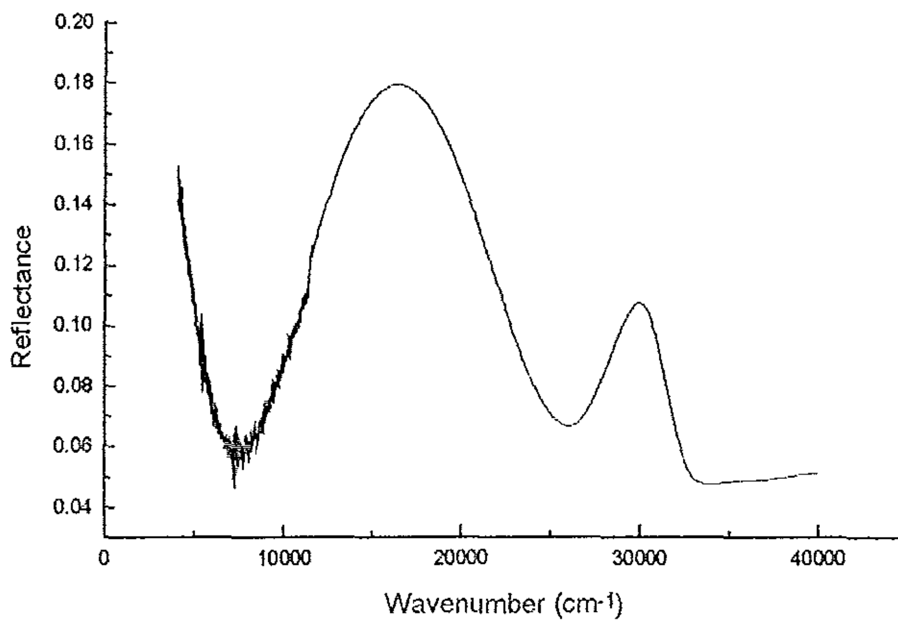

Figure 5.2 Reflectance spectrum of the TCO sample.

In figure 5.1 the transmittance spectrum of the TCO sample is displayed. In the infrared region for the wavenumbers between 4107.5cm^{-1} and 7814.9cm^{-1} the transmittance of the TCO sample increases from 0.478 to 0.825. In figure 5.2 the reflectance spectrum of the TCO sample is displayed. The reflectance in this spectral region drops from 0.153 to 0.056. In the infrared spectral region and at the beginning of the visible spectral region for the wavenumbers between 7814.9cm^{-1} to 16841.8cm^{-1} the transmittance decreases from 0.825 to 0.8 (figure 5.1) and the reflectance in this spectral region increases from 0.056 to 0.18 (figure 5.2). At the high energy end of the visible spectral region and in the ultraviolet spectral region for the wavenumbers 16841.8cm^{-1} upto 27480.6cm^{-1} the transmittance increases from 0.8 to 0.86 (figure 5.1) and the reflectance in this spectral region decreases from 0.18 to 0.063 (figure 5.2). In the ultraviolet spectral region for the wavenumbers 27480.6cm^{-1} up to 34089.6cm^{-1} the transmittance decreases from 0.86 to 0.008 (figure 5.1) and in this spectral region the reflectance increases from 0.063 to 0.103 (figure 5.2). Below 34089.5cm^{-1} the transmittance and the reflectance become a constant value of 0.049 until the wavenumbers reaches 40,000cm^{-1}.

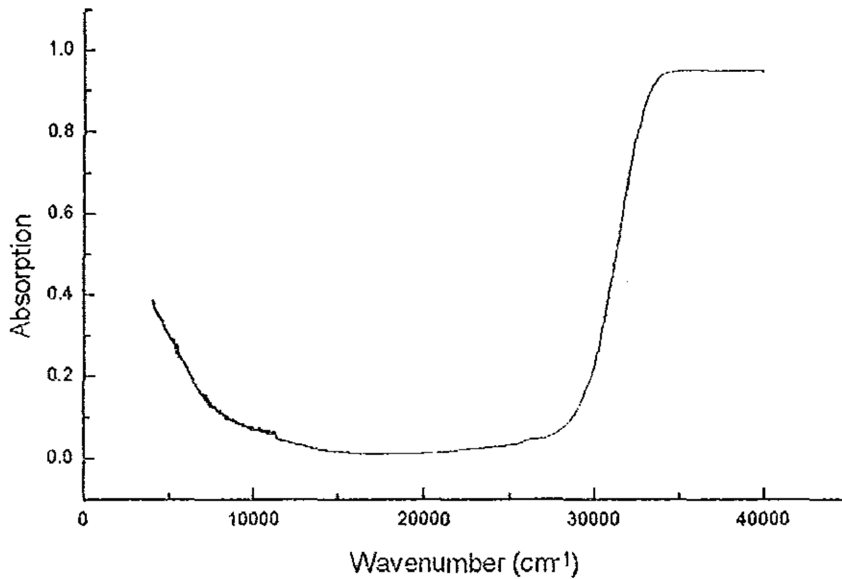

Figure 5.3 Absorption spectrum of the TCO sample calculated from the corresponding transmittance (figure 5.1) and reflectance spectrum (figure 5.2).

The reflectance, the transmittance and the absorption are add up to 1. Therefore in this layer system there is an absorption band throughout the whole spectrum from 4,000cm^{-1} upto 40,000cm^{-1} (figure 5.3). However, the absorption is dominant in the ultraviolet spectral region above the wavenumber of 32,800cm^{-1}.

5.2 TCOP sample

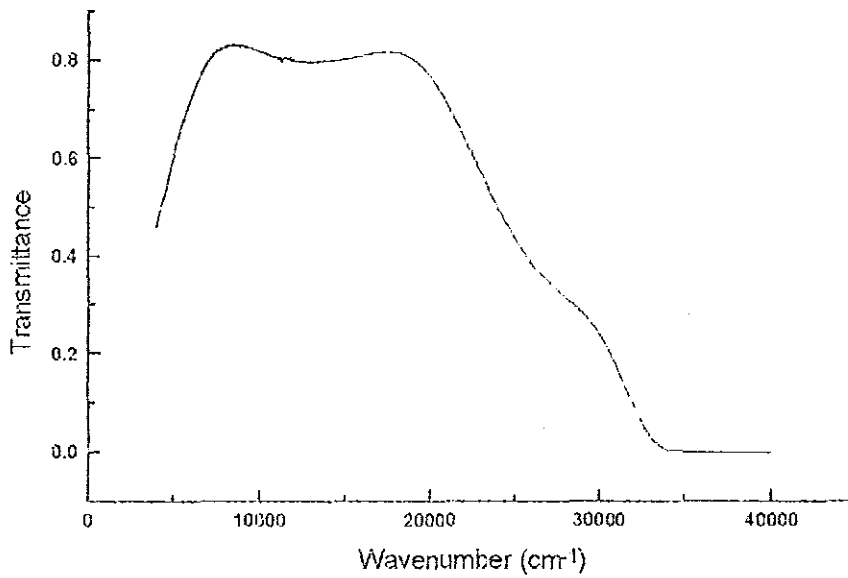

Figure 5.4 Transmittance spectrum of the TCOP sample (consisting of a glass substrate and a coated transparent conducting oxide layer with an additional p-doped a-Si:H layer).

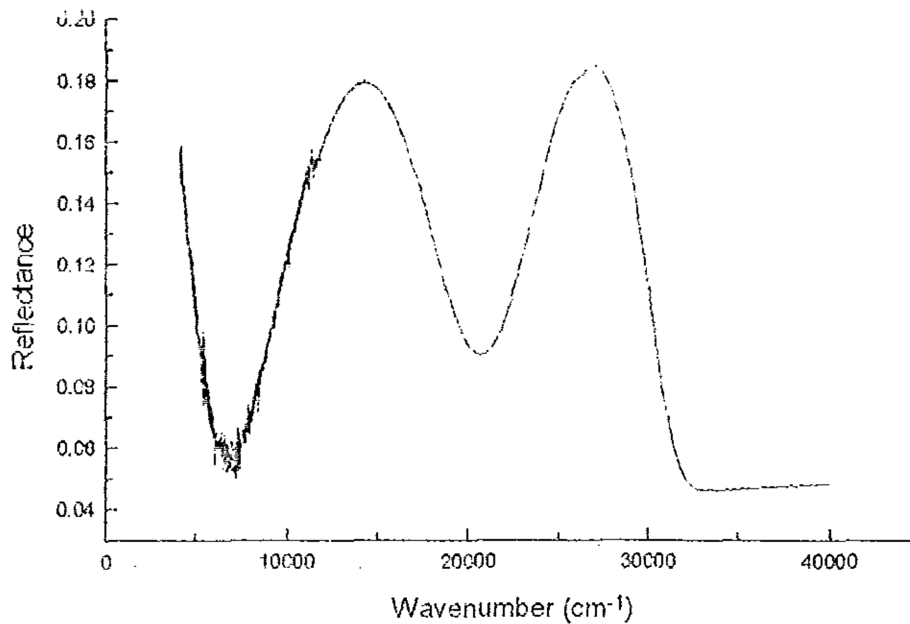

Figure 5.5 Reflectance spectrum of the TCOP sample.

In figure 5.4 the transmittance spectrum of the TCOP sample is displayed. In the infrared region for the wavenumbers between 4268.7cm^{-1} to 7331.3cm^{-1} the transmittance of the TCOP sample increases from 0 .478 to 0.825 and for the same spectral region the reflectance decreases from 0.153 to 0.056 (figure 5.5). In the infrared spectral region and visible spectral region for the wavenumbers between 7331.34cm^{-1} to 14104.5cm^{-1} the transmittance decreases from 0.825 to 0.805 (figure 5.4) and for the same spectral region the reflectance increases from 0.056 to 0.184 (figure 5.5). In the visible spectral region of the spectrum in the wavenumbers region between 14104.5cm^{-1} to 20100cm^{-1} the transmittance of the TCOP sample increases from 0.805 to 0.813 (figure 5.4) and for the same spectral region the reflectance decreases from 0.184 to 0.086 (figure 5.5).

In the ultraviolet spectral region for wavenumbers from 20,100 cm^{-1} to 26997cm^{-1} the transmittance decreases from 0.813 to 0.37 (figure 5.4) and for the same spectral region the reflectance increases from 0.086 to 0.184 (figure 5.5).

In the ultraviolet spectral region for the wavenumbers range between 26997cm^{-1} to 33605.9cm^{-1} the transmittance decreases from 0.321 to 0.019 and for the same spectral region the reflectance decreases from 0.184 to 0.049. For the wavenumbers region between 33605.9cm^{-1} to 40,000cm^{-1} the transmittance and reflectance will be 0.019 and 0.049 respectively.

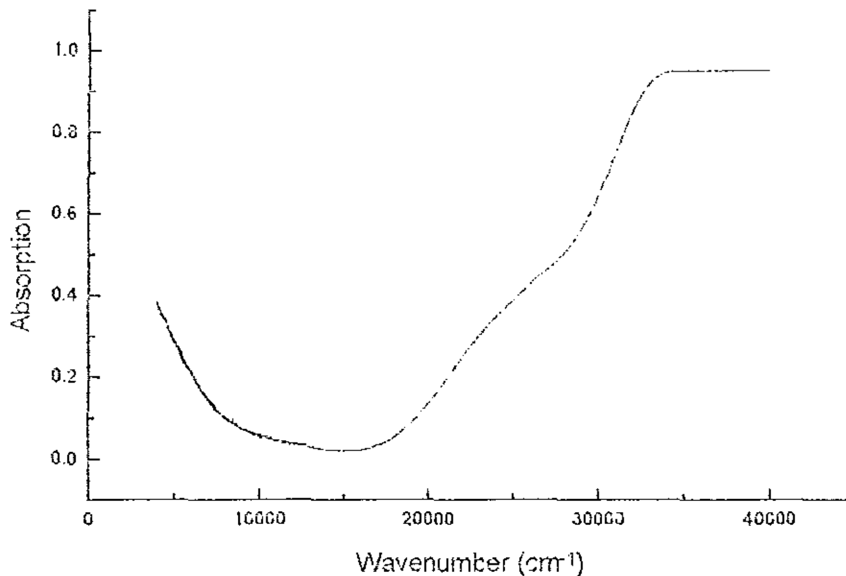

Figure 5.6 Absorption spectrum of the TCOP sample calculated from the corresponding transmittance (figure 5.4) and reflectance spectrum (figure 5.5).

As the reflectance, the transmittance and the absorption for the same sample sum up to 1, in comparison to the absorption spectrum of the TCO sample (figure 5.3), the absorption band observed in the TCOP sample (figure 5.6) is spectrally broader and reaches far more in the visible spectrum. Up to 20,000cm^{-1} the addition of the p-layer hence increases the absorption of the whole layer stack system into the visible region. The other difference between the TCO and TCOP samples is observed in the reflectance spectra. The peak value of the reflectance in the ultraviolet spectral region for the TCO sample is smaller (0.103) than that of the peak value of the reflectance of the TCOP sample (0.184). Also the reflectance spectrum of the TCOP sample shows a pronounced double maxima structure which exists due to internal multiple reflection in the 15nm thick p-layer.

5.3 TCOPI1 sample

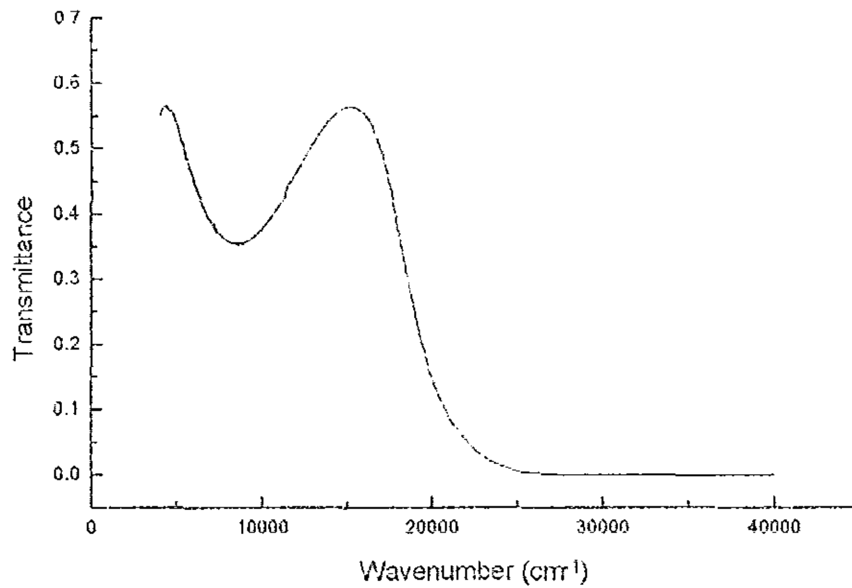

Figure 5.7 Transmittance spectrum of the TCOPI1 sample (consisting of a glass substrate, a coated TCO layer, an additional coated p-doped a-Si:H and an additional I-layer).

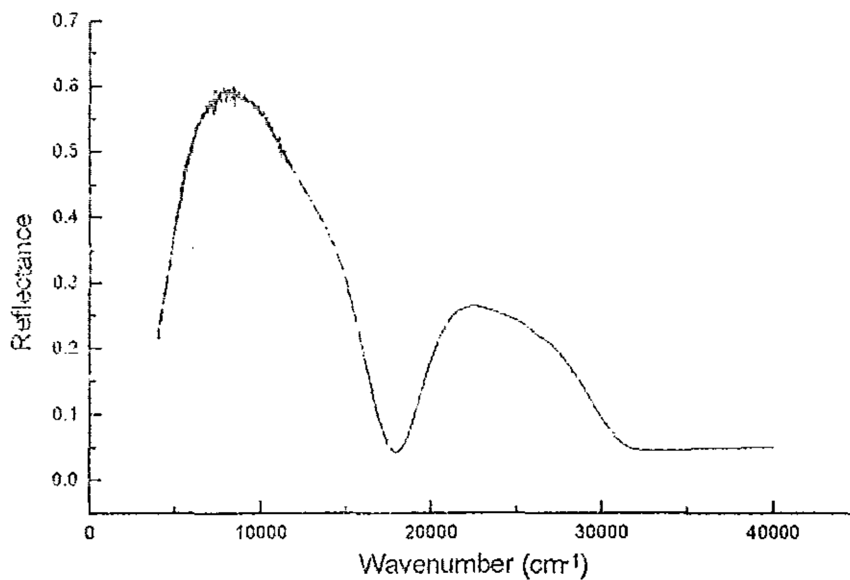

Figure 5.8 Reflectance spectrum of the TCOPI1 sample.

In figure 5.7 the transmittance spectra of the TCOPI1 sample is displayed. In the infrared spectral region for wavenumbers from 4107.5cm^{-1} to 8620.9cm^{-1} the transmittance decreases from 0.556 to 0.355 and for the same spectral region the reflectance of the sample increases from 0.243 to 0.59 (figure 5.8). In the infrared and visible spectral regions for the wavenumber range from 8298.5cm^{-1} to 17808.9cm^{-1} the transmittance increases from 0.355 to 0.567 (figure 5.7) and for the same spectral region the reflectance of the layer stack decreases from 0.59 to 0.041 (figure 5.8). In the visible and ultraviolet spectral region in the wavenumber range from 17909.9 cm^{-1} to 23611.9 cm^{-1} the transmittance decreases from 0.567 to 0.03 (figure 5.7) and for the same spectral region the reflectance of the layer stack increases from 0.041 to 0.265 (figure 5.8).

In the ultraviolet spectral region for the wavenumbers from 23611.9 cm^{-1} to 40,000 cm^{-1} the transmittance is zero (figure 5.7). In the ultraviolet spectral region for the wavenumbers from 23611.9 cm^{-1} to 31188.1 cm^{-1} the reflectance decreases from 0.265 to 0.053 and for the same figure in the ultraviolet region for the wavenumbers from 31188.1cm^{-1} to 40,000 cm^{-1} the value of the reflectance is a constant value of 0.053 (figure 5.8).

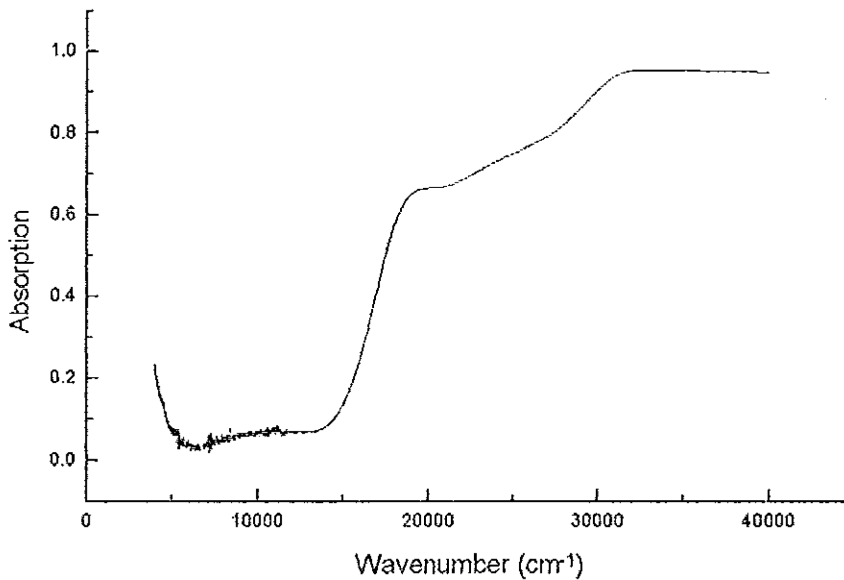

Figure 5.9 Absorption spectrum of the TCOPI1 sample calculated from the corresponding transmittance (figure 5.7) and reflectance spectra (figure 5.8).

Since the reflectance, transmittance and absorption are add up to 1, throughout the whole spectrum there is an absorption band in the layer stack system which reaches far into the visible spectral region up to 15000cm^{-1} (figure 5.9). In comparison to the TCOP sample the TCOPI1 sample has an additional intrinsic a-Si:H layer introduced to the layer stack system. Due to the absorption of this layer in the ultraviolet spectral range the transmittance is negligible and the reflectance is very small. As the I-layer is introduced, the transmittance of the layers can be neglected in the ultraviolet region and also the reflectance of the layer system is very small in this region where the absorption band dominates. The other difference between the reflectance of the TCOP and TCOPI1 sample is that the maximum peak value for the reflectance spectrum of the TCOP layer is less than that of the TCOPI1 layer.

5.4 TCOPI2 sample

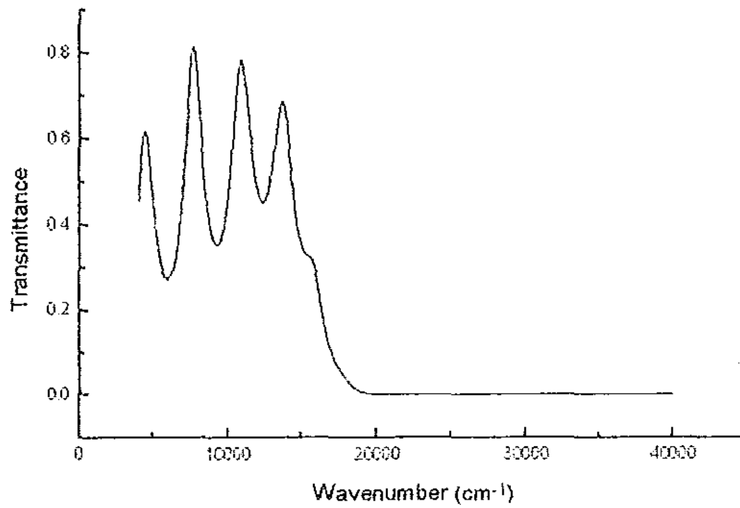

Figure 5.10 Transmittance spectrum of the TCOPI2 sample (consisting of a glass substrate, a coated transparent conducting oxide layer and an additional coated p doped a-Si:H layer and an additional I-layer).

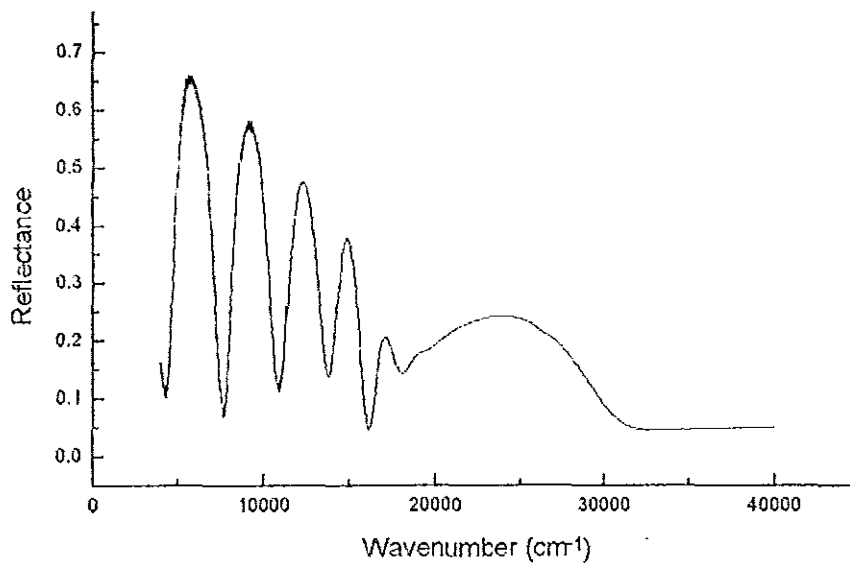

Figure 5.11 Reflectance spectrum of the TCOPI2 sample

In figure 5.10 the transmittance spectrum of the TCOPI2 sample is displayed. In the infrared spectral region for the wavenumber region from 4107.5cm^{-1} upto 4429.9cm^{-1} the transmittance of the TCOPI2 sample increases from 0.467 to 0.61 and the reflectance decreases from 0.176 to 0.12 (figure 5.11). In the infrared spectral region for the wavenumber region from 4429.9cm^{-1} to 6041.8cm^{-1} the transmittance of the TCOPI2 sample decreases from 0.612 to 0.265 (figure 5.10) and the reflectance increases from 0.12 to 0.646 (figure 5.11). In the infrared spectral region for the wavenumber region from 6041.8cm^{-1} to 7653.7cm^{-1} the transmittance of the TCOPI2 layer increases from 0.265 to 0.802 (figure 5.10) and the reflectance decreases from 0.646 to 0.075 (figure 5.11). In the infrared spectral region for the wavenumber region from 7653.7cm^{-1} to 9265.7cm^{-1} the transmittance of the TCOPI2 layer decreases from 0.802 to 0.343 (figure 5.10) and the reflectance increases from 0.075 to 0.58 (figure 5.11). In the infrared spectral region for the wavenumber region from 9265.7cm^{-1} to 10877.6cm^{-1} the transmittance of the TCOPI2 sample increases from 0.343 to 0.78 (figure 5.10) and the reflectance of the sample decreases from 0.58 to 0.109. At the high energy end of the infrared region in the wavenumber region from 10877.6cm^{-1} upto 12489.6cm^{-1} the transmittance decreases from 0.78 to 0.44 (figure 5.10) and the reflectance increases from 0.109 to 0.478 (figure 5.10). In the visible region for wavenumbers from 12489.6cm^{-1} upto 13671.9cm^{-1} the transmittance increases from 0.44 to 0.69 (figure 5.10) and the reflectance decreases from 0.478 to 0.131 (figure 5.11).

In the visible spectral region in the wavenumber region from 13671.9cm^{-1} up to 14907.5cm^{-1} the transmittance decreases from 0.69 to 0.36 and in figure 5.8 for the same region the reflectance increases from 0.131 to 0.38. In figure 5.10 in the visible spectral region for wavenumber from 14907.5cm^{-1} upto 15874.6cm^{-1} the transmittance

decreases from 0.355 to 0.321 (figure 5.10) and the reflectance decreases from 0.38 to 0.053 (figure 5.11). In the visible spectral region for wavenumber from 15874.6cm^{-1} upto 20065.67cm^{-1} the transmittance decreases from 0.321 to 0 (figure 5.10) and in the visible spectral region for wavenumber from 15874.6cm^{-1} upto 17002.9cm^{-1} the reflectance increases from 0.053 to 0.198 (figure 5.11). For the same figure in the visible spectrum region for wavenumber from 17002.9cm^{-1} upto 17970.2cm^{-1} the reflectance decreases from 0.198 to 0.131 (figure 5.11). At the high energy end of the visible and the beginning of the ultraviolet region in the wavenumber region from 17970.2cm^{-1} upto 24740.3cm^{-1} the reflectance increases from 0.131 to 0.254 . In the ultraviolet region for wavenumber from 24740.3cm^{-1} to 31026.9cm^{-1} the reflectance decreases from 0.254 to 0.041 (figure 5.11). The spectral maxima positions of the transmittance spectrum are always complementary with the spectral minima positions of the corresponding reflectance spectrum. As the wavenumber increases above 20065.7cm^{-1} the transmittance will be zero and the reflectance decreases and approaches to 0.041.

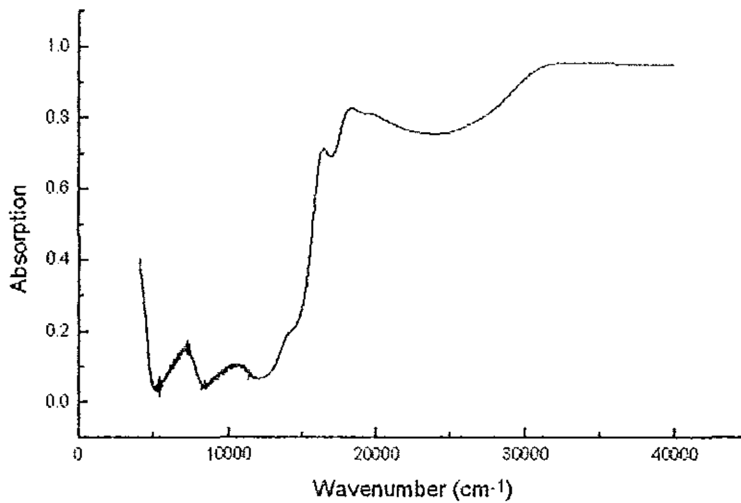

Figure 5.12 Absorption spectrum of TCOPI2 sample calculated from the corresponding transmittance (figure 5.10) and reflectance spectra (figure 5.11).

Since the transmittance, the reflectance and the absorption for the same sample add up to 1, there is an absorption band in the layer stack system (figure 5.12). For the TCOPI2 sample the absorption dominates in the ultraviolet spectral region and makes the transmittance and reflectance in this spectral region to be very small. As the intrinsic layer thickness increases up to 380nm, in comparison to the TCOPI1 sample where the intrinsic layer is 50nm thick, internal multiple interferences inside the intrinsic a-Si:H layer takes place and a larger number of interference fringes are observed in the reflectance and transmittance spectra in comparison to the TCOPI1 sample. Also as the intrinsic layer thickness increases the absorption in the ultraviolet and visible spectral region increases.

6. COMPUTER SIMULATION OF TRANSMITTANCE AND REFLECTANCE SPECTRA OF a-Si:H MULTILAYER STACKS

6.1 SCOUTFIT computer programme

SCOUT stands for Spectroscopic Objects and Utilities and is a Windows application for CAOS. CAOS is an abbreviation for Computers Assisted Optical Spectroscopy, which is an approach to the interpretation of optical spectra by computer simulation. A direct simulation of optical spectra has to be based on the macroscopic response of matter to electric fields which is given by the dielectric function of the material. Hence, SCOUT provides a wide and growing variety of possibilities to define dielectric functions:

- Definition of dielectric functions on the basis of simple models : constant susceptibility, Drude model for free carriers, harmonic oscillator model for interband transitions (band gap) (see chapter 2, pp 5).

The SCOUTFIT computer programme is used to determine the layer thickness and the dielectric function of a single layer as well as multilayer stacks with an input of measured transmittance and reflectance spectra at normal incidence or at different angles. The step by step introduction of the parameters to the SCOUTFIT programme to compare measured reflectance or transmittance spectra to the simulated ones will give the exact result. The simulation is done with a small variation of the parameters corresponding to the given transmittance and reflectance spectra until there is an agreement between the measured spectra and the simulated curves. In applying the SCOUTFIT programme the following procedures are required:

a) Define the layer stack.

b) Define the dielectric function models of all materials inside the layers or layer stacks.

c) Define the experimental set up of the spectrum which is imported into the programme.

In doing so a continuous interaction of the parameters will be done by rough estimation of the parameters until the automatic fit becomes successful. The fitting process is done both by hand and automatically. [1]

By using the SCOUTFIT programme based on the above rules the parameters of the dielectric functions applied to the spectra (discussed in chapter 5) are determined.

6.2 Computer simulation of the reflectance spectrum of the TCO sample

The TCO sample consists of a glass substrate coated with a transparent conducting Oxide (TCO) layer. Therefore the layer structure used by the computer simulation inside the SCOUTFIT programme is among a half space of Vacuum, a simple layer of glass, followed by a simple layer of TCO which again is enclosed by a half space of vacuum. The reflectance spectrum imported into the programme is displayed in figure 5.2. The dielectric function used to simulate the individual layers is for the half space vacuum the fixed dielectric function value of $\varepsilon=1$, for the glass layer the harmonic oscillator model to simulate the band gap of glass, consists of the resonance frequency, the oscillator strength, the distribution width, the damping constant and the dielectric background value and finally the glass layer thickness (see chapter 2, pp 5). For the TCO layer the Drude model is introduced to the computer simulation to simulate the influence of the free carriers of this layer. The fitting parameters include the plasma frequency, the dielectric background of this material and the TCO layer thickness. The layer stack structure and the list of dielectric function used are shown in table 6.1.

Layer structure	Layer	Modell dielectric function
Half space	Vacuum	ε=1
simple layer	Glass	Harmonic oscillator + dielectric background
simple layer	TCO	Drude model + dielectric background
Half space	Vacuum	ε=1

Table 6.1 The layer stack of the TCO sample and the SCOUTFIT dielectric function models.

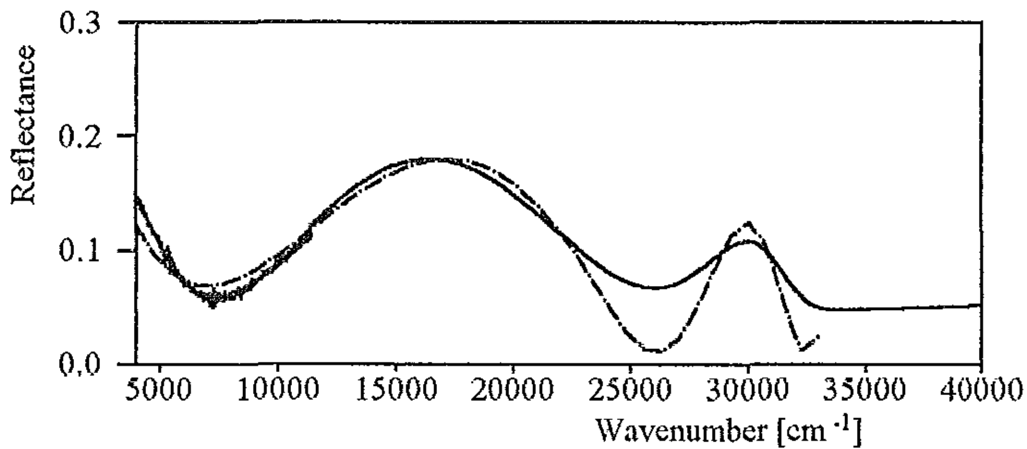

Figure 6.1 The reflectance (dark line) and the SCOUTFIT simulated spectra (dotted line) of the Glass/TCO sample.

Figure 6.1 displays the result of the SCOUTFIT programme for the reflectance of the TCO sample. The dotted line shows the computer simulated spectra and the dark line shows the measured reflectance spectra. The least square value of the difference between the two spectra is 0.0004846. The simulated optical parameters are tabulated below in table 6.2.

Dielectric function model parameters	Values	Dimension
Glass: dielectric background: Real part	2.13	
Glass: band gap: distribution width	50.06	cm^{-1}
Glass: band Gap: damping	2770.9983	cm^{-1}
Glass: band gap : oscillator strength	1095.5513	cm^{-1}
Glass: band Gap: resonance frequency	39675.3	cm^{-1}
Glass: layer thickness	956.4194	μm
TCO: free carriers: damping	456.5405	cm^{-1}
TCO: free carriers: plasma frequency	8920.502	cm^{-1}
TCO: dielectric background: real part	3.6786	
TCO: layer thickness	0.0619	μm

Table 6.2 SCOUTFIT optical parameters for the TCO sample simulated with a reflectance spectrum.

6.2 Computer simulation for the transmittance of The TCO sample

The dielectric functions used are the same as for the TCO sample in the simulation of the reflectance spectrum. The transmittance spectrum imported into the programme is displayed in figure 5.1. The list of dielectric function and the layer stack are tabulated in table 6.3.

Layer structure	Layer	Model dielectric function
Halfspace	Vacuum	ε=1
Simple layer	Glass	Harmonic oscillator + dielectric background
Simple layer	TCO	Drude model + dielectric background
Half space	Vacuum	ε=1

Table 6.3 The layer stack of the TCO sample and the SCOUTFIT dielectric function models.

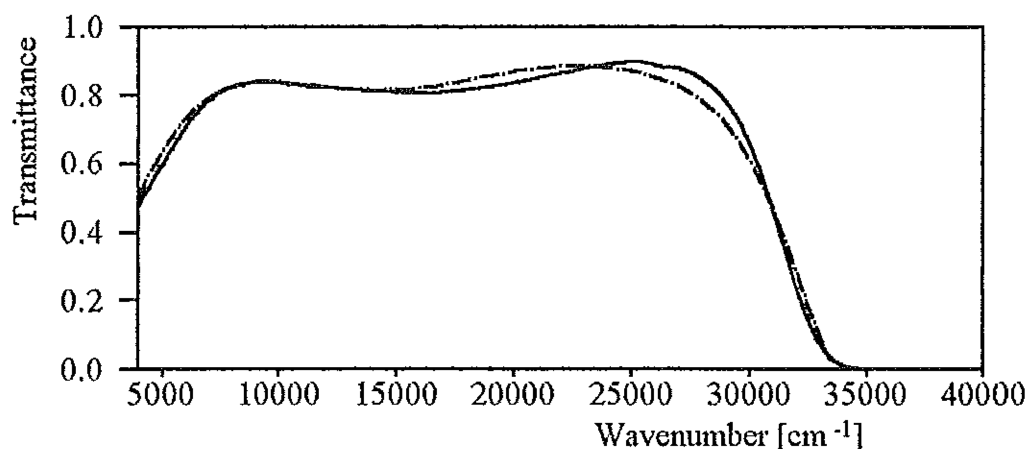

Figure 6.2 The transmittance (dark line) and the SCOUTFIT simulated spectra (dotted line) of the TCO sample.

Figure 6.2 displays the result of the SCOUTFIT programme for the transmittance of the TCO sample. The dotted line shows the computer simulated spectrum and the

dark line shows the measured transmittance spectrum. The least square value for the difference between the two spectra is 0.0008019 and the simulated optical parameters are tabulated in table 6.4.

Dielectric function model	Values	Dimension
Glass: dielectric background: real part	2.21	
Glass: band gap: distribution width	1731.6219	cm^{-1}
Glass: band gap: damping	654.4803	cm^{-1}
Glass: band gap: oscillator strength	429.3679	cm^{-1}
Glass: band gap: resonance frequency	37268.3945	cm^{-1}
Glass: layer thickness	1022.956	μm
TCO: free carriers: plasma frequency	13000	cm^{-1}
TCO: dielectric background: real part	3.6749	
TCO: free carriers: damping	985.1888	cm^{-1}
TCO: layer thickness	0.0688	μm

Table 6.4 SCOUTFIT optical parameters of the TCO sample simulated with the transmittance spectrum.

6.4 Computer simulation for the reflectance of the TCOP sample

The TCOP sample consists of a glass substrate coated with a TCO layer and an additional coated p doped a-Si:H layer. The dielectric function used are the same as that of the TCO sample with an additional Drude model and dielectric background for the p layer. The reflectance spectrum imported into the programme is displayed in figure 5.5. The layer stack and the list of dielectric function models are tabulated in table 6.5.

Layer structure	Layer	Model dielectric function
Half space	Vacuum	$\varepsilon=1$
Simple layer	Glass	Harmonic oscillator + dielectric background
Simple layer	TCO	Drude model + dielectric background
Simple layer	P-layer	Drude model + dielectric background
Half space	Vacuum	$\varepsilon=1$

Table 6.5 The layer stack of the TCOP sample and the SCOUTFIT dielectric function models.

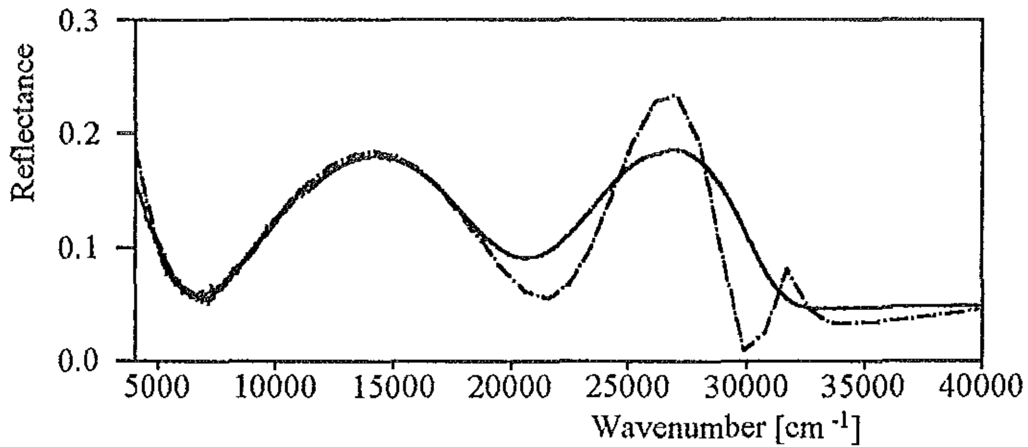

Figure 6.3 The reflectance (dark line) and the SCOUTFIT simulated spectra (dotted line) for the TCOP sample.

Figure 6.3 displays the result of the SCOUTFIT programme fit for the reflectance of the TCOP sample. Where the dark line shows the reflectance spectrum and the dotted line shows the computer simulated spectrum due to the tabulated parameters. The least square value for the difference between the two spectra is 0.0007848. The simulated optical parameters are tabulated in table 6.6.

Dielectric function model parameters	Values	Dimension
Glass: band gap: distribution width	1604.3713	cm^{-1}
Glass: band gap: damping	2012.0564	cm^{-1}
Glass : band gap: oscillator strength	815.9837	cm^{-1}
Glass : band gap : resonance frequency	39907.328	cm^{-1}
Glass : layer thickness	1017.6191	μm
Glass: dielectric background: real part	2.3328	
TCO : free carriers : damping	488.9775	cm^{-1}
TCO : free carriers : plasma frequency	12807.739	cm^{-1}
TCO : dielectric background: real part	3.7848	
TCO : layer thickness	0.0695	μm
P-layer: free carriers: damping	15030.111	cm^{-1}
P-layer: free carriers: plasma frequency	10042.433	cm^{-1}
P-layer: dielectric background: real part	11.65	
P-layer: layer thickness	0.015	μm

Table 6.6 SCOUTFIT optical parameters of the TCOP sample simulated with a reflectance spectrum.

6.5 Computer Simulation of the transmittance of the TCOP sample

The sample and the dielectric function models used are the same as for the TCOP sample in the simulation of the reflectance spectrum 6.3. The transmittance spectrum imported into the programme is displayed in figure 5.4. The layer stack and the list of dielectric function are shown in table 6.7.

Layer structure	Layer	Model dielectric function
Half space	Vacuum	ε=1
Simple layer	Glass	Harmonic oscillator + dielectric background
Simple layer	TCO	Drude model + dielectric background
Simple layer	P-layer	Drude model + dielectric background
Half space	Vacuum	ε=1

Table 6.7 The layer stack of the TCOP sample and the SCOUTFIT dielectric function models.

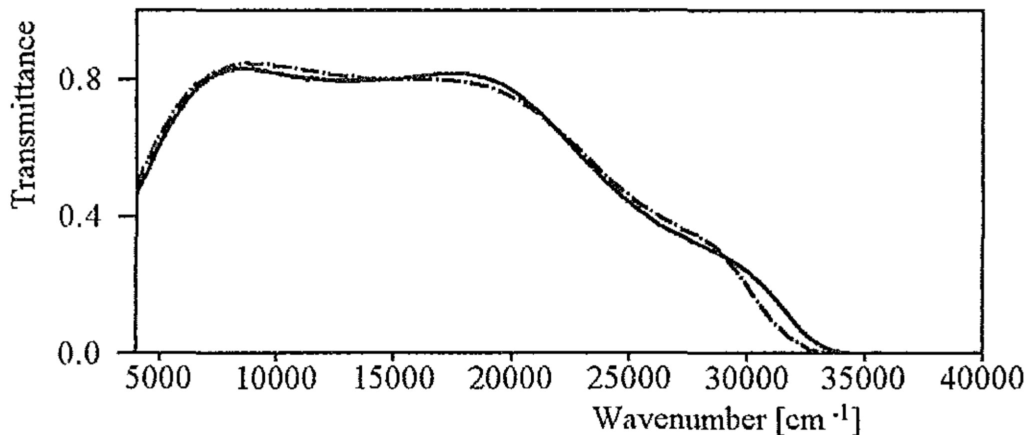

Figure 6.4 The transmittance (dark line) and the SCOUTFIT simulated spectra (dotted line) of the TCOP sample.

Figure 6.4 displays the result of the SCOUTFIT programme for the transmittance of the TCOP sample. The dotted line shows the computer simulated spectra and the

dark line shows the measured transmittance spectra. The least square value of the difference between the two spectra is 0.0006256. The simulated optical parameters are tabulated in table 6.8.

Dielectric function model parameters	Values	Dimension
Glass: dielectric background: real part	2.3112	
Glass: band gap: distribution width	2000.91	cm^{-1}
Glass: band gap: damping	1851.9138	cm^{-1}
Glass: band gap: oscillator strength	581.5004	cm^{-1}
Glass: band gap: resonance frequency	38293.875	cm^{-1}
Glass: layer thickness	1092.2369	μm
TCO: free carriers: damping	472.9692	
TCO: free carriers: plasma frequency	14000	cm^{-1}
TCO: dielectric background: real part	3.9178	
TCO: layer thickness	0.0703	μm
P-Layer: dielectric background: real part	11.7353	
P-layer: free carriers: damping	635.5182	cm^{-1}
P-layer: free carriers: plasma frequency	18000	cm^{-1}
P-layer: layer thickness	0.0141	μm

Table 6.8 SCOUTFIT optical parameters of the TCOP sample simulated with a transmittance spectrum.

The TCOPI1 sample consists of a glass substrate, coated with a TCO layer and is additional coated with p doped a-Si:H layer and an additional i-layer. The dielectric function models used are the same as for TCOP sample with an additional harmonic oscillator model and dielectric background for the i-layer. The reflectance spectrum imported into the programme is displayed in figure 5.8. The list of dielectric function models and the layer stack are shown in table 6.9.

Layer structure	Layer	Model dielectric function
Half space	Vacuum	ε=1
Simple layer	Glass	Harmonic oscillator + dielectric background
Simple layer	TCO	Drude model + dielectric background
Simple layer	P-layer	Drude model + dielectric background
Simple layer	I-layer	Harmonic oscillator + dielectric background
Half space	Vacuum	ε=1

Table 6.9 The layer stack of the TCOPI1 sample and the SCOUTFIT dielectric function models.

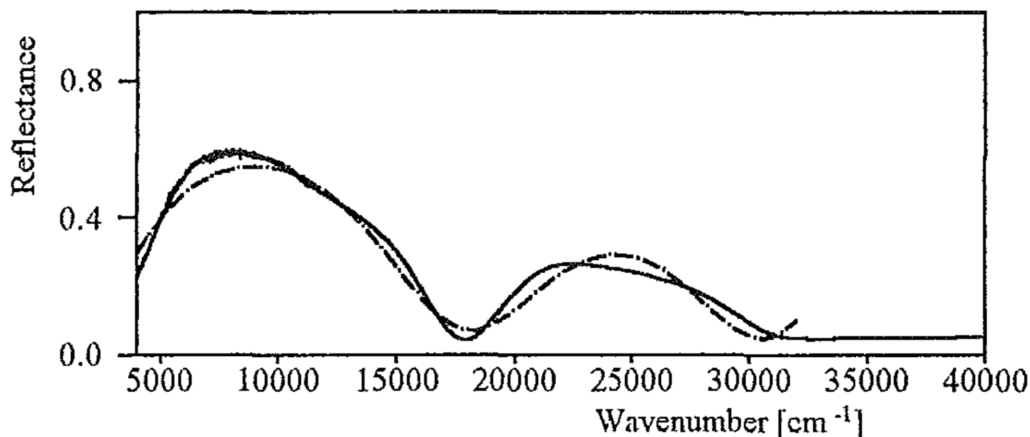

Figure 6.5 The reflectance (dark line) and the SCOUTFIT simulated spectra (dotted line) for the TCOPI1 sample.

Figure 6.5 displays the result of the SCOUTFIT programme fit for the reflectance of the TCOPI1 sample, where the dotted line shows the computer simulated spectrum and the dark line shows the measured reflectance spectrum. The least square value of the difference between the two spectra is 0.0012459. The simulated optical parameters are tabulated in table 6.10.

Dielectric function model parameters	Values	Dimension
Glass: dielectric background: real part	2.1106	
Glass: band gap: distribution width	1289.8541	cm^{-1}
Glass: band gap: damping	865.499	cm^{-1}
Glass: band gap: oscillator strength	452.6223	cm^{-1}
Glass: band gap: resonance frequency	41149	cm^{-1}
Glass: Layer thickness	1073.7852	μm
TCO: free carriers: damping	504.1816	cm^{-1}
TCO: free carriers: plasma frequency	4357.8354	cm^{-1}
TCO: dielectric background: real part	4.4749	
TCO: layer thickness	0.0629	μm
P-layer: dielectric background: real part	13.0777	
P-layer: free carriers: damping	402.1344	cm^{-1}
P-layer: free carriers: plasma frequency	915.8302	cm^{-1}
P-layer: layer thickness	0.0167	μm
I-layer: dielectric background: real part	5.46	cm^{-1}
I-layer: layer thickness	0.0405	μm
I-layer: band gap: resonance frequency	15812.3076	
I-layer: band gap: oscillator strength	439.7651	cm^{-1}
I-layer: band gap: damping	46.4987	cm^{-1}

Table 6.10 SCOUTFIT optical parameters of the TCOPI1 sample simulated with a reflectance spectrum.

6.7 Computer simulation of the transmittance of the TCOPI1 sample

The dielectric function models used are the same as that of the TCOPI1 sample. The transmittance spectrum imported into the programme is displayed in figure 5.7. The layer stack and the list of dielectric function are shown in table 6.11.

Layer structure	layer	Model dielectric function
Half space	Vacuum	ε=1
Simple layer	Glass	Harmonic oscillator + dielectric background
Simple layer	TCO	Drude model + dielectric background
Simple layer	P-layer	Drude model + Dielectric background
Simple layer	I-layer	Harmonic oscillator + dielectric background
Half space	Vacuum	ε=1

Table 6.11 The layer stack of the TCOPI1 sample and the SCOUTFIT dielectric function models.

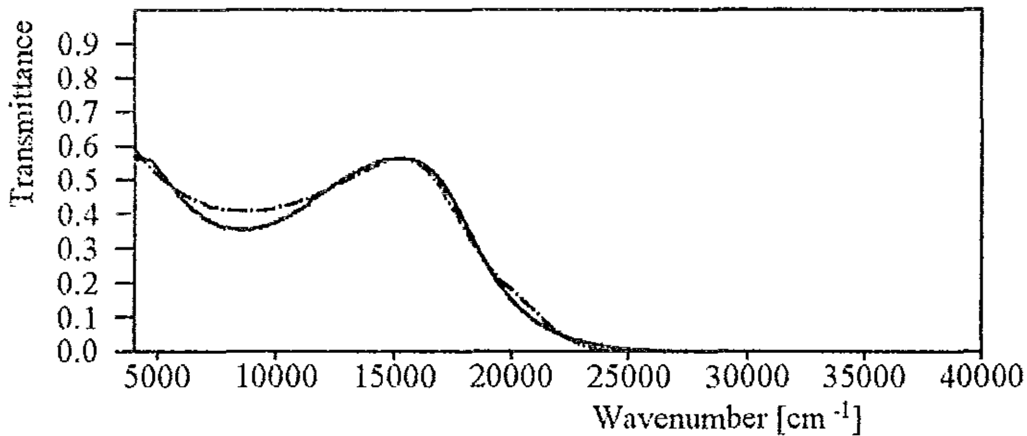

Figure 6.6 The transmittance (dark line) and the SCOUTFIT simulated spectra (dotted line) for the TCOPI1 sample.

Figure 6.6 displays the result of the SCOUTFIT programme for the transmittance of the TCOPI1 sample. Where the dotted line shows the simulated spectrum and the

dark line shows the transmittance spectrum. The least square value for the difference of the two spectra is 0.0006605 and the values of the optical parameters are tabulated in table 6.12.

Dielectric function model	Values	Dimension
Glass: dielectric background: real part	2.25	
Glass: band gap: distribution width	1517.69	cm^{-1}
Glass: band gap: damping	1529.1465	cm^{-1}
Glass: band gap: oscillator strength	955.1711	cm^{-1}
Glass: band gap: resonance frequency	34889.0605	cm^{-1}
Glass: layer thickness	1045.0153	μm
TCO: free carriers: damping	583.6895	cm^{-1}
TCO: free carriers: plasma frequency	4512.6982	cm^{-1}
TCO: dielectric background: real part	3.64	
TCO: layer thickness	0.069	μm
P-layer: dielectric background: real part	11.6355	
P-layer: free carriers: damping	548.3973	cm^{-1}
P-layer: free carriers: plasma frequency	1285.1846	cm^{-1}
P-layer: layer thickness	0.0113	μm
I-layer: dielectric background: real part	5.39	
I-layer : layer thickness	0.0479	μm
I-layer: band gap: resonance frequency	13999.3496	cm^{-1}
I-layer: band gap: damping	46.5418	cm^{-1}

Table 6.12 SCOUTFIT optical parameters of the TCOPI1 sample simulated with a transmittance spectrum.

6.8 Computer simulation of the reflectance spectra of the TCOPI2 sample.

The TCOPI2 sample consists of a glass substrate coated with a TCO layer and is additional coated with a p and i doped a-Si:H layer and the thickness of the i layer in this case is approximately 380nm. The dielectric functions used are the same as that of the TCOPI1 sample. The reflectance spectrum imported into the programme is displayed in figure 5.11. The list of dielectric function are shown in table 6.13.

Layer structure	Layer	Model dielectric function
Half space	Vacuum	ε=1
Simple layer	Glass	Harmonic oscillator + dielectric background
Simple layer	TCO	Drude model + dielectric background
Simple layer	P -layer	Drude model + dielectric background
Simple layer	I-layer	Harmonic oscillator + dielectric background
Half space	Vacuum	ε=1

Table 6.13 The layer stack of the TCOPI2 sample and the SCOUTFIT dielectric function models.

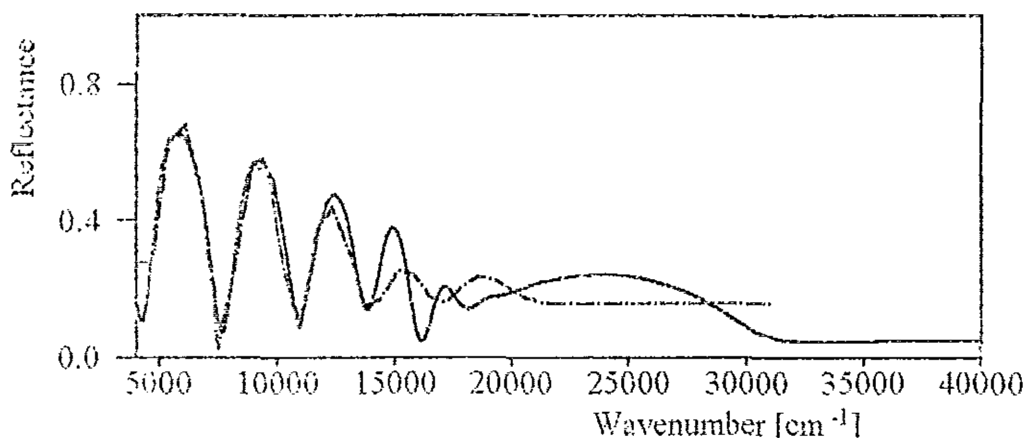

Figure 6.7 The reflectance (dark line) and the SCOUTFIT simulated spectra (dotted line) of the TCOPI2 sample.

Figure 6.7 displays the result of the SCOUTFIT programme fit for the reflectance of the TCOPI2 sample. The dotted line shows the computer simulated spectra and the dark line shows the measured reflectance spectra. The least square value of the difference between the two spectra is 0.0042678. The simulated optical parameters of the TCOPI2 layer are tabulated in table 6.14.

Dielectric function model parameters	Values	Dimension
Glass: dielectric background: real part	2.2036	
Glass: band gap: distribution width	1211.4092	cm^{-1}
Glass: band gap: damping	2069.4312	cm^{-1}
Glass: band gap: oscillator strength	631.3893	cm^{-1}
Glass: band gap: resonance frequency	38988.6752	cm^{-1}
Glass: layer thickness	1098.4385	µm
TCO: free carriers: damping	420.8046	cm^{-1}
TCO: free carriers: plasma frequency	1000.5662	cm^{-1}
TCO: dielectric background: real part	4.2836	
TCO: layer thickness	0.068	µm
P-layer: dielectric background: real part	10.7988	
p-layer: free carriers: damping	491.6903	cm^{-1}
p-layer: free carriers: plasma frequency	1208.9017	cm^{-1}
P-layer: layer thickness	0.016	µm
I-layer: dielectric background: real part	5.48	
I-layer: layer thickness	0.3942	µm
I-layer: band gap: resonance frequency	13723.3984	cm^{-1}
I-layer: band gap: oscillator strength	1050.6021	cm^{-1}
I-layer: band gap: damping	40.0607	cm^{-1}

Table 6.14 SCOUTFIT optical parameters of the TCOPI2 sample simulated with the reflectance spectrum.

6.9 Computer simulation of the transmittance of the TCOPI2 sample

The dielectric function models used are the same as for the TCOPI2 sample used in the reflectance simulation in section 6.7. The transmittance spectrum imported into the programme is displayed in figure 5.10. The list of dielectric function models and the layer stack are tabulated in table 6.15.

Layer structure	Layer	Model dielectric function
Half space	Vacuum	$\varepsilon=1$
Simple layer	Glass	Harmonic oscillator + dielectric background
Simple layer	TCO	Drude model + dielectric background
Simple layer	P-layer	Drude model + dielectric background
Simple layer	I-layer	Harmonic oscillator + dielectric background
Half space	Vacuum	$\varepsilon=1$

Table 6.15 The layer stack of the TCOPI2 sample and the SCOUTFIT dielectric function models.

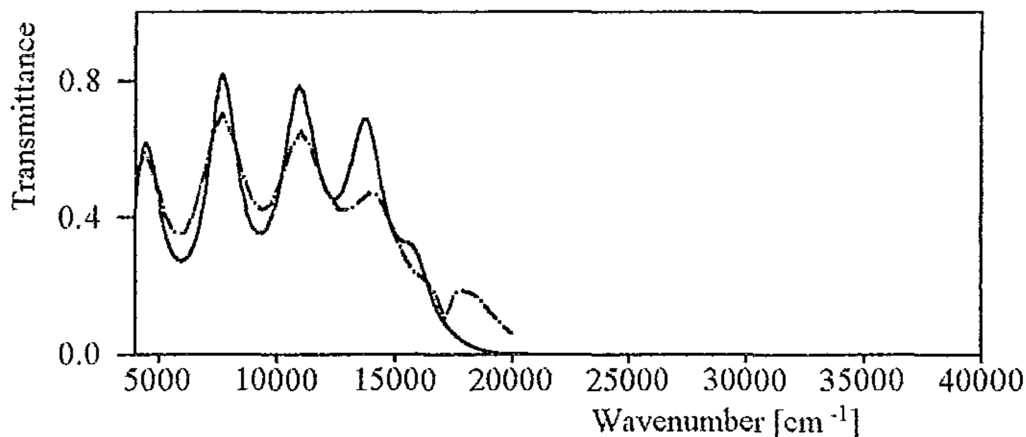

Figure 6.8 The transmittance (dark line) and the SCOUTFIT simulated spectra (dotted line) of the TCOPI2 sample.

Figure 6.8 displays the result of the SCOUTFIT programme fit for the transmittance of the TCOPI2 sample, where the dotted line shows the computer simulated spectrum and the dark line shows the measured transmittance spectrum. The least square value of the difference of the two spectra is 0.0058662 and the optical parameters obtained from the simulation are tabulated in table 6.16.

Dielectric function model parameters	Values	Dimension
Glass: dielectric background: real part	2.125	
Glass: band gap: distribution width	1509.4189	cm^{-1}
Glass: band gap: damping	3265.3584	cm^{-1}
Glass: band gap: oscillator strength	1124.4586	cm^{-1}
Glass: band gap: resonance frequency	35687.93	cm^{-1}
Glass: layer thickness	987.54	μm
TCO: free carriers: damping	1641.2438	
TCO: free carriers: plasma frequency	12907.4561	cm^{-1}
TCO: dielectric background: real part	3.8869	
TCO: layer thickness	0.0795	μm
P-layer: dielectric background: real part	11.6252	
P-layer: free carriers: damping	692.4374	cm^{-1}
P-layer: free carriers: plasma frequency	7995.1724	cm^{-1}
P-layer: layer thickness	0.015	μm
I-layer: dielectric background: real part	5.64	
I-layer: layer thickness	0.393	μm
I-layer: band gap: resonance frequency	16944.5932	cm^{-1}
I-layer: band gap: oscillator strength	2500.01	cm^{-1}
I-layer: band gap: damping	106.9138	cm^{-1}

Table 6.16 SCOUTFIT optical parameters of the TCOPI2 sample simulated with the transmittance spectrum.

7. DISCUSSION OF THE OPTICAL PROPERTIES OF a-Si:H MULTILAYER STACKS

7.1 Discussion of the layer thickness

In this section the optical properties of the observed a-Si:H multilayer stacks obtained from the SCOUTFIT programme in section 6 will be discussed. Table 7.1 shows thee layer thickness of the TCO, TCOP, TCOPI1 and TCOPI2 samples for the transmittance and the reflectance spectrum. Also the average values of the layer thickness of the samples and the reference value obtained from the references are tabulated.

Layer	Samples									
	TCO		TCOP		TCOPI1		TCOPI2			
	Refl. (μm)	Tran. (μm)	Refl. (μm)	Tran. (μm)	Refl. (μm)	Tran. (μm)	Refl. (μm)	Tran. (μm)	Average(μm)	Reference (μm)
Glass	956.42	1,022.96	1,017.62	1,092.24	1,073.52	1,045.02	1,098.44	987.54	1,036.7	1000 [18]
TCO	0.0619	0.0688	0.0695	0.0703	0.0629	0.069	0.068	0.0795	0.0687	0.07 [18]
P	-	-	0.015	0.0141	0.0167	0.0113	0.016	0.015	0.0147	0.015 [18]
I_1	-	-	-	-	0.045	0.0479	-	-	0.0465	0.050 [18]
I_2	-	-	-	-	-	-	0.394	0.393	0.3935	0.38 [18]

Table 7.1 The thickness of each layer. (where Refl. stands for reflectance and Tran. stands for transmittance).

The average value of the layer thickness of glass obtained from the transmittance and reflectance spectra fitted by the SCOUTFIT programme is 1036.72 μm whereas the reference value obtained from [18] is 1000 μm, thus the deviation is 3.672 %. The average value of the layer thickness of the TCO layer obtained from the transmittance and the reflectance spectra fitted by the SCOUTFIT programme is 0.0687μm and the value from the reference [18] , is 0.07μm, thus the deviation is 1.857 %.

The average value of the thickness of the p- doped a-Si:H layer obtained from the reflectance and the transmittance spectra of the SCOUTFIT programme fit is 0.0147μm and the value obtained in the reference [18] is 0.015μm. Thus the deviation is 2 %. The average value of the thickness of the I_1 doped a-Si:H layer obtained from the reflectance and the transmittance spectra fitted by the SCOUTFIT programme is 0.0465μm where as the value obtained from reference [18] is 0.05μm. Thus the deviation of the layer thickness between the two values is 7 %.

The average value of the thickness of I_2 - doped a-Si:H layer obtained from the reflectance and transmittance spectra fitted by the SCOUTFIT programme is 0.3935 μm where as the value obtained in the reference [18] has a layer thickness value of 0.380μm. Thus the deviation of the layer thickness is 3.553 %.

For the layer thickness the deviation between the fitted value and the reference values is not more than 7 %. This is a quite good correlation and proves that the fitting of optical transmittance and reflectance spectra with the SCOUTFIT programme gives a reliable source to determine the layer thickness of the thin film layer components.

7.2 Discussion of the optical parameters

The other properties that will be discussed is the dielectric background which is denoted by ε_{∞} and is mathematically expressed by the equation (3.4). In table 7.2 the average value and the reference value of the obtained dielectric background constants and the band gap resonance frequency parameters for TCO, TCOP, TCOPI1 and TCOPI2 are tabulated.

Dielectric function model parameters	Average value	Reference	Deviation
Glass: dielectric background: real part	2.21	2.25 [17]	1.78%
Glass: band gap: distribution width	1364.42 cm^{-1}		
Glass: band gap: damping	1877.36 cm^{-1}		
Glass: band gap: oscillator strength	760.76 cm^{-1}		
Glass: band gap: resonance frequency	38232.45cm^{-1}	37908cm^{-1}[17]	0.86%
TCO: free carriers: damping	694.2 cm^{-1}		
TCO: free carriers: plasma frequency	8938.37 cm^{-1}		
TCO: dielectric background: real part	3.92	3.8 [29]	3.158%
P-layer: dielectric background: real part	11.75	11.7 [28]	0.427%
P-layer: free carriers: damping	712.21 cm^{-1}		
P-layer: free carriers: plasma frequency	6574.59cm^{-1}		
I_1-layer: dielectric background: real part	5.43	5.17 [15]	5.02%
I_1-layer: band gap: resonance frequency	14905.83 cm^{-1}	13873cm^{-1}[34]	7.445%
I_1-layer: band gap: oscillator strength	559.28 cm^{-1}		
I_1-layer: band gap: damping	46.52 cm^{-1}		
I_2-layer: dielectric background: real part	5.56	5.17 [18]	7.544%
I_2-layer: band gap: resonance frequency	15334 cm^{-1}	13873cm^{-1} [34]	10.53%
I_2-layer: band gap: oscillator strength	1775.31 cm^{-1}		
I_2-layer: band gap: damping	73.49 cm^{-1}		

Table 7.2 The average value of the dielectric function model parameters obtained

For the glass layer a simple oscillator model was used to simulate the optical band gap of the material. The obtained fitted band gap resonance frequency can be compared with the reference value. The differènce is only 0.68 %, so that the band gap energy of glass is successfully obtained. The overall dielectric background used has a deviation of 1.78 % from the reference value.

In the simulation process the simple harmonic oscillator model together with the dielectric background model is used for glass and can successfully describe the measured reflectance and transmittance spectra.

In the simulation of the TCO layer the Drude model and the dielectric background model are used to determine the dielectric background and the free carriers damping and plasma frequency. The obtained value of the dielectric background as compared to the referred value has a deviation of 3.158 %. Thus, the simple models used in this simulation gives a good result.

For the P- doped a-Si:H layer the simulation is done by using the Drude model with the free carriers damping and plasma frequency as parameters and the dielectric background model is used to determine the dielectric background. The obtained value of the dielectric background compared to the reference value has a deviation of 0.427 %. Thus, using the Drude model and the dielectric background model for simulation of the optical properties of the TCO layer gives a very good result.

The next layer which is simulated is the I-layer with a layer thickness of 50 nm and 380 nm by using the oscillator model and the dielectric background model to determine the dielectric background and the band gap resonance frequency. The obtained dielectric background for the I- layer of thickness 50nm has a deviation of 5.02 % and for the I-layer of thickness 380nm has a deviation of 7.544 %, also the

obtained band gap energy for the 50nm layer thickness has a deviation of 7.445 % and for the I-layer of thickness 380nm the deviation of the band gap energy as compared to the referred value has a deviation of 10.531 %.

The cause for the deviation of the obtained values by the SCOUTFIT simulation programme with the reference values is that really simple models were used in this determination which of course can only approximately simulate the complex layer stack system.

Additional reasons for the obtained deviations between fitted and reference values are the experimental errors and the inhomogeneous of the sample thickness which could be up to 3 %. However the executed computer simulation of the measured transmittance and reflectance spectra of a-Si:H layer stacks can provide valuable information of the layer thickness and optical parameters which are in the same accuracy region obtained with other simulation methods like the Hishikawa's relation method and the Tauc's plot method. [2, 3]

8. REFERENCE

[1] W. Theis, **The SCOUT Through CAOS, A System For Doing Optics By Computer**, computer programme manual, Aachen (1994) pp. 1-70.

[2] A. Abdi,Thesis (AAU), **Optical Characterization Of Thin Films For Solar Cell Application**, Addis Ababa (1995).

[3] E. Bekele,Thesis (AAU), **Optical Characterization Of Thin Film Solar Cells**, Addis Ababa (1996).

[4] N. W. Ashcroft, N. D. Marmin, **Solid State Physics**, CBS publishing Asia ltd, Philadelphia (1987) pp. 2-25.

[5] L. D.Partain (ed.), **Solar Cells And Their Applications**, Wiley-Series in Microwave and Optical Engineering, New York (1995) pp. xxi - xxiii and 1-20.

[6] Y. Hamakawa, **Solar And Wind Technology**, Appl. Phys. vol. 6 No. 3 (1989) pp. 241-246.

[7] B. Harbecke, **Coherent And Incoherant Reflection And Transmission Of Multilayer Structures**, appl. phys. B39 (1986) pp. 165-170.

[8] Perkin Elmer, **Lambda 19 Spectrometer manual**, user documentation, volume 1 of 3.

[9] Perkin Elmer, **Lambda 19 Spectrometer manual**, user documentation, volume 2 of 3.

[10] Perkin Elmer, **Lambda 19 Spectrometer manual**, user documentation, volume 3 of 3.

[11] B. Harbecke, **Application Of Fourier's Allied Integrals To The Kramer's - Kronig Transformation Of Reflectance Data**, appl. phys. A 40 (1986) pp. 151-158.

[12] A. R. Forouhi, I. Bloomer, **Optical Properties Of Crystalline Semiconductors And Dielectrics**, Phys. Rev. vol. 38, No. 3 (1988) pp. 1865-1873.

[13] R. Saeng -Udom, W. Kusian and B. Bullemer, **Optical Modelling Of Amorphous Silicon Solar Cells**, Siemens AG, corporate research and development, Munich (1990) pp. 331-334.

[14] B. O. Seraphin, **Amorphous Silicon Solar Cells**, optical science center, university of Arizona Tucson (1990) pp. 1-20.

[15] A. R. Forouhi, I. Bloomer, **Optical Dispersion Relations For Amorphous Semiconductors And Amorphous Dielectrics**, phys. rev. vol. 34, No.10, (1986) pp. 7018-7026.

[16] A. R. Forouhi and I. Bloomer, **Calculation Of Optical Constants, n And k, In The Interband Region**, hand book of optical constants of solids II, acadamic press, (1991) pp. 151-175.

[17] D. A. Neaman, **Semiconductor Physics And Devices**, Irwin, Boston (1992) pp. 615-625.

[18] T. Eickhoff, H. Stiebig, **Modellierung Der Spektralen Empfindlichkeit Von a-Si:H Solarzellen**, Photovoltaik 3, Forschungsverbund Sonnenenergie, Themen 95/96, Koeln (1996) pp. 90 -180.

[19] T. Markvart (ed.), **Solar Electricity**, Wiley, Chichester (1994) pp.21-69

[20] C. Kittel, **Introduction To Solid State Physics**, 6th edition, Wiley, New York (1986) pp. 548-553.

[21] P. Grosse (editer), **Advances In Solid State Physics**, Vieweg, Braunschweig (1983) pp. 41-44.

[22] M. Evenschor, P. Grosse, W. Theis, **Optics Of Two-Phase Composites**, Vibrational spectroscopy, vol. 1, (1990) pp. 173-177.

[23] W. Theis, The Use Of Effective Medium Theories In Optical Spectroscopy, Festkoerperprobleme 33, edited by R. Helbig, Vieweg, Braunschweig (1994) pp. 75-78.

[24] K. D. Leaver, B. N. Chapman, **Thin Films**, Imperial College, London, (1971) pp. 90-180.

[25] B. O. Seraphin, **Solid State Physics Aspects Of Solar Energy Conversion**, International Atomic Energy Agency, SMR, 20/44 Vienna (1977) pp. 301-327.

[26] T. Kamai, N. Hata and A. Matsuda, **Deposition And Extensive Light Soaking Of Highly Pure Hydrogenated Amorphous Silicon**, vol.305, Umzono Tsukuba (1996) pp. 2785-2790.

[27] S. J. Fonash, **Solar Cell Device Physics**, Academic press, London (1981) pp. 1-5.

[28] R. J. Schwartz, G. B. Turner, J. W. Park, J. L. Gray, **Physics Of Amorphous Semiconductor Devices**, vol. 763 (1987) pp. 126.

[29] R. Plattner, W. Stetter, P. Kohler, **Transparent Conductive Tin-Oxide Layers For Thin Film Solar Cell**, Siemens Forsch. -U. Entwickel. -Ber. Bd. 17 (1988) No. 3, pp. 126.

[30] W. Kruehler, **Duennschicht-Solar Zellen aus Amorphen Halbleitern**, edited by D. Meissner, Vieweg, Braunschweig, (1993).

[31] Y. Hishikawa, N. Nakamura, S. Tsuda, S. Nakano, Y. Kishi and Y. Kuwano, **Interference-Free Determination Of The Optical Absorption Coefficient And The Optical Gap Of Amorphous Silicon Thin Films**, Japanese journal of applied physics, vol. 30, No. 5 (1991) pp.1008-1014.

[32] F. Leblanc, J. Perrin, E. Cornil, J. Schmitt, **Experimental Characterization And Optical Modeling Of Absorption And Light Trapping In a-Si:H Solar Cells On Textured TCO**, material research society processed vol. 258 (1992) pp. 917-918.

[33] C. F. Klingshirn, **Semiconductor Optics**, Springer, Berlin (1995) pp.23-93.